Monthly Notices
of the
ROYAL ASTRONOMICAL SOCIETY

MNRAS **490,** 927–946 (2019)
Advance Access publication 2019 September 16

doi:10.1093/mnras/stz2589

A Bayesian *Fermi*-GBM short GRB spectral catalogue

J. Michael Burgess [1,2★] Jochen Greiner,[1,2] Damien Bégué[1] and Franceso Berlato[1,3]

[1]*Max-Planck-Institut für extraterrestrische Physik, Giessenbachstrasse 1, D-85748 Garching, Germany*
[2]*Excellence Cluster Universe, Technische Universität München, Boltzmannstraße 2, D-85748 Garching, Germany*
[3]*Physik Department, Technische Universität München, James-Franck-Strasse 1, D-85748 Garching, Germany*

Accepted 2019 September 11. Received 2019 July 17; in original form 2018 October 5

ABSTRACT

Inspired by the confirmed detection of a short gamma-ray burst (GRB) in association with a gravitational wave signal, we present the first Bayesian *Fermi*-Gamma-ray Burst Monitor (GBM) short GRB spectral catalogue. Both peak flux and time-resolved spectral results are presented. Data are analysed with the proper Poisson likelihood allowing us to provide statistically reliable results even for spectra with few counts. All fits are validated with posterior predictive checks. We find that nearly all spectra can be modelled with a cut-off power law. Additionally, we release the full posterior distributions and reduced data from our sample. Following our previous study, we introduce three variability classes based on the observed light-curve structure.

Key words: methods: data analysis – catalogues – gamma-ray burst: general.

1 INTRODUCTION

The *Fermi* Gamma-ray Burst Monitor (GBM; Meegan et al. 2009) is the most prolific detector of short gamma-ray bursts (GRBs). Over its 10 yr mission beginning in 2008 July, GBM has detected over 300 short GRBs. Long believed to be the by-product of binary neutron star mergers, the recent association of GW 170817 (Abbott et al. 2017a,b) with the short GRB 170817A (Abbott et al. 2017c; Goldstein et al. 2017) has made the study of GBM short GRB population properties pertinent. First of all, the low luminosity combined with otherwise typical spectral properties of short GRBs demands an explanation of the physical emission mechanism (e.g. Bégué, Burgess & Greiner 2017; Kasliwal et al. 2017). Next, given the detection rate within the Laser Interferometer Gravitational-Wave Observatory (LIGO) second observing run (O2) of $R = 1540^{+3200}_{-1220}$ Gpc^{-3} yr^{-1} (Abbott et al. 2017a) and consistent predictions from population studies (e.g. Chruslinska et al. 2018), it is obvious to ask for the detection of similar events in the GBM archival data that remained unrecognized as nearby mergers (e.g. Burgess et al. 2017). This also includes the question as to whether or not it is possible to identify nearby binary neutron star mergers based on just the gamma-ray data and potential optical/near-infrared (NIR) follow-up? Last but not least, questions like a clear distinctive separation from long-duration GRBs (based on the hardness–duration, lags, and temporal properties), the physical interpretation of soft tails, or the relations to magnetars (e.g. Rowlinson et al. 2014) all require input from a homogeneously deduced sample of spectral parameters.

Past GBM spectral catalogues (e.g. Goldstein et al. 2012; Gruber et al. 2014; Yu et al. 2016) have utilized maximum likelihood methods to provide spectral properties of GRBs to the community. Herein, we have invoked Bayesian analysis to extract both the temporal and spectral properties of short GRBs. This allows for the injection of our prior beliefs about the properties of short GRBs that results in the ability to uniformly model the data across various photon functions and properly select between spectral models. Additionally, we provide the results of our analysis and data reduction to the community to encourage follow-up studies.

This paper is organized as follows. First, we describe the sample selection and data reduction. Next, we detail out spectral fitting procedure and the catalogue distributions. Finally, we briefly discuss the implications of our results.

2 SAMPLE SELECTION

The *Fermi* Science Support Center[1] (FSSC) provides public data from the *Fermi* mission including GBM burst data.[2] Additionally, the GBM public GRB burst catalogue[3] provides up-to-date durations and background selections for all triggers classified as GRBs since the beginning of the mission.

Using these data bases, we selected all GRBs with a T_{90} duration less than 7 s and retrieved the time-tagged event (TTE) data, response matrices, and background selections for detectors with a viewing angle less than 60° from the reported source location.

★ E-mail: jburgess@mpe.mpg.de

[1]https://fermi.gsfc.nasa.gov/ssc/
[2]https://heasarc.gsfc.nasa.gov/FTP/fermi/data/gbm/bursts/
[3]https://heasarc.gsfc.nasa.gov/W3Browse/fermi/fermigbrst.html

The time span of this selection is from 2008 July 14 to 2017 August 18. While we will eventually use GRBs with a duration less than 2 s, we obtain those with a longer T_{90} because we will use a different duration measure as detailed in Section 3. GBM releases response matrices in two forms. Some GRBs have responses for a single time interval (RSP) and others have responses determined for multiple time intervals to account for the slewing of the spacecraft (RSP2). If RSP2 files are available, we utilize these over the RSP files. However, the short durations of these GRBs means that there should be little difference between the use of RSPs and RSP2s.

The original sample includes 543 GRBs before data reduction. Because of issues with background selections and lack of significant signal, some GRBs were removed from the sample resulting in 321 short GRBs and 525 time-resolved spectra. The details of the data reduction are discussed in the following section.

3 METHODOLOGY

Following our work in Burgess et al. (2017) and Greiner et al. (2016), we apply a uniform methodology for background fitting, temporal binning, and time-resolved source selection. Each step is detailed in the following paragraphs.

3.1 Data reduction

For each GRB in our sample, an off-source background interval is selected using the intervals identified in the GBM online catalogue. Using these intervals, a series of four polynomials of increasing degree (from 0–3) is fit to the total rate in time. The likelihood for the fit is unbinned Poisson and as nested models, a likelihood ratio test (LRT) is applied using the likelihoods of each polynomial fit to find the more parsimonious degree of polynomial. A threshold of 10 in delta log likelihood is used to determine if an increase in polynomial degree is significant. With the degree determined, a polynomial of the same degree is fit to each of the 128 pulse height amplitude (PHA) channels to estimate the background model for the rate in that channel. The background will be integrated in time over each source interval. As the background estimation is the result of a maximum likelihood fit, the errors are assumed to be Gaussian distributed. Thus, when calculating the statistical error on the background for each channel, the covariance matrix of the background fit is propagated into the temporal integration resulting in our background error, $\sigma_{\rm b}$.

With the background fitted, we apply Bayesian blocks (Scargle et al. 2013) to the temporally unbinned source interval for each detector ($T_0 - 5 + 10$ s) with a chance probability parameter of $p_0 = 0.01$. The background model is used to shift the background from a non-homogeneous Poisson process to a homogeneous one. If no change points (significant changes of the Poisson rate) are inferred, the GRB is discarded from the sample. The detector light curve with the highest rate significance over the background is selected and its inferred change points are mapped to all other detectors. We note that the appropriate significance measure to use is via a likelihood ratio similar to that derived by Li & Ma (1983). However, that likelihood is derived for the significance of one Poisson rate over another. Since our determined background model possesses Gaussian errors, the appropriate likelihood ratio is that where we seek an excess over a Gaussian background rate. Thus, we determine significance via the method of Vianello (2018).

The intervals for spectral analysis are now selected by retaining all bins with a significance greater than 3σ. For each bin, the background model is integrated over the bin's time bounds and a source and background are exported to PHA files. Similarly, if the GRB has an RSP2 file, a weighted response matrix is calculated and exported.

3.2 Spectral analysis

For each temporal bin, we fit both a Band function (Band, Matteson & Ford 1993; Greiner et al. 1995),

$$F(E) = K \begin{cases} \left(\frac{E}{E_{\rm piv}}\right)^{\alpha} {\rm e}^{-\frac{E}{E_{\rm cut}}} & E \leq (\alpha-\beta)E_{\rm cut}, \\ \left(\frac{E}{E_{\rm piv}}\right)^{\beta} {\rm e}^{(\beta-\alpha)} \left[\frac{(\alpha-\beta)E_{\rm cut}}{E_{\rm piv}}\right]^{\alpha-\beta} & E > (\alpha-\beta)E_{\rm cut}, \end{cases} \quad (1)$$

and a cut-off power law (CPL) function,

$$F(E) = K \left(\frac{E}{E_{\rm piv}}\right)^{\alpha} \exp\left(-\frac{E}{E_{\rm cut}}\right). \quad (2)$$

Both functions are parametrized in terms of a cut-off energy ($E_{\rm cut}$) rather than a νF_ν-peak energy to reduce correlations between the peak and the low-energy spectral index (α). However, we compute the νF_ν-peak energy ($E_{\rm p}$) and report it for comparisons to previous results. We do not fit a simple power-law model to the data because we expect a spectral peak somewhere within the GBM energy range as higher spectral peaks have never been observed. When power-law models are fit to short GRBs, it is typically found that the photon spectral index is $\sim > -1.5$ which would imply a peak outside the GBM spectral window (Gruber et al. 2014). As we discuss below, we mitigate this with our prior choices. For all parameters except the photon model normalization, we adopt weakly informative priors. Our priors are guided by past GRB catalogues, including GBM's, but not derived from fits to those distributions. Moreover, our priors are derived from the assumption that a spectral peak lies within the GBM energy window. Thus, our priors are not coming from the data used herein. Additionally, as we have essentially created new data via our temporal selections and proper background fitting, we would not be in danger of violating any principles of Bayesian analysis. We choose a normal prior on the cut-off energy of both the Band and CPL functions centred at 200 keV and truncated at 10 keV. Thus, unless the data are more informative than the prior, we impose that a spectral peak exists in the GBM spectral window. The following prior choices were used:

$$\alpha \sim \mathcal{N}(\mu = -1, \sigma = 0.5), \quad (3)$$

$$E_{\rm cut} \sim \mathcal{N}(\mu = 200, \sigma = 300), \quad (4)$$

$$\beta \sim \mathcal{N}(\mu = -2.25, \sigma = 0.5). \quad (5)$$

The spectra are fit via a Poisson–Gaussian likelihood to account for Poisson distributed total counts and Gaussian distributed background estimate[4] (Arnaud, Smith & Siemiginowska 2011; Greiner et al. 2016). This is defined as

$$-2\log L = 2\sum_{i=1}^{N} M_i + t_{\rm s} f_i - S_i \log(M_i t_{\rm s} f_i) + \frac{1}{2\sigma_{{\rm b},i}^2}(B_i - t_{\rm b} f_i)^2 - S_i(1 - \log S_i), \quad (6)$$

[4]This is known as PGSTAT in XSPEC.

where N is the number of spectral bins, M_i, S_i, and B_i are the predicted, detected, and background counts in the ith bin, respectively, σ_{b_i} is the Gaussian uncertainty on the background, t_s and t_b are the source and background durations, and f_i is a function of the background counts resulting from the profiling of the statistic. This profile likelihood removes the need for a background spectral model by essentially assuming a parameter in each spectral bin and profiling it out, i.e. maximizing the likelihood for the background model. This requires at least one background count in each spectral bin and thus, we bin the spectra to achieve this goal. However, this rarely reduces the number of bins by more than one or two.

To account for systematics in the GBM responses, we scale all responses except one by a normalization constant, a so-called effective area correction. A similar procedure was used in Yu et al. (2016). The GBM responses are claimed accurate to with 10 per cent (Bissaldi et al. 2009), and therefore we place a Cauchy prior centred at unity with a 10 per cent standard deviation on these normalization constants. The Cauchy prior is informative in its tails but allows for some lack of certainty around the mean. These corrections will be marginalized into our spectral parameter posteriors. A constant, energy-independent correction likely does not account for all complex misspecification of the GBM photon-to-count conversion process that is present in the responses. Nevertheless, without access to the full spacecraft model[5] or a comprehensive GBM detector in-flight calibration paper, we must make an assumption that the linear correction to the effective area will suffice.

Finally, to perform the spectral fit, we sample the posterior with the MULTINEST algorithm (Feroz, Hobson & Bridges 2009). For each fit, 600 live points are used.[6] MULTINEST ceases to sample when a tolerance on the marginal likelihood integral has been achieved. Hence, we record the value of the marginal likelihood (Z) for each fit. Because of our use of informative priors (Bartlett 1957; Strachan & Dijk 2003), we can employ model selection between the Band and CPL functions via marginal likelihood ratios. This equates to choosing the more parsimonious model given the data and parameter values.[7] Model selection is performed in each time interval allowing for the spectral model to evolve within a burst.

All temporal and spectral analysis is carried out with the Multi-Mission Maximum Likelihood framework (3ML; Vianello et al. 2015). The results are stored in Flexible Image Transport System (FITS) 'analysis results' files that are readable by 3ML or any normal FITS reader. They contain information regarding the spectral model and the full posterior of all parameters. Each file can be used to fully set up the analysis for replication. Additionally, we propagate the spectral fit into an energy flux (F_E) calculation integrated over the 10 keV–1 MeV energy range resulting in a marginal distribution for the energy flux. Note that via the analysis result FITS files, the fluxes can be recomputed over any energy range.

In the previous work, the authors have argued that a more complicated spectral fitting algorithm should be invoked to account for systematics in the locations of GRBs (see the BAyesian Location Reconstruction of GRBs (BALROG); Burgess et al. 2018) and that physical photon models provide better insight into the emission mechanism of GRBs (Burgess, Ryde & Yu 2015; Burgess 2017). However, works on the systematics in location are ongoing, and as we note in Bégué et al. (2017), the emission mechanism of short GRBs requires further modelling. Therefore, with the confirmation of binary neutron star mergers as at least one progenitor of short GRBs, we find it pertinent to proceed with the classical photon models in order to provide the modelling community with an empirical view of the spectra. Additionally, we will utilize the publicly available data products such as the standard responses.

4 RESULTS

From our temporal binning and spectral fitting results, we provide the joint and individual parameter distributions for our sample. We consider the total duration of the emission as the interval from the beginning of the first to ending of the last Bayesian block from our temporal analysis. We note that this is quite different than the typical T_{90} (Koshut et al. 1995) used for GRB durations and thus, we simply call this the duration of the GRB. Our duration does not account for the detector response as it is calculated in count space, however, we do not compare our results to previous duration measures for any interpretation. Moreover, duration measures are somewhat arbitrarily performed in different energy ranges, and differ across instruments. What is perhaps most important is how relative durations vary within a sample. A comparison of T_{90} and our duration is shown in Fig. 1. The deviation at short durations between the two measures is the result of many of the GBM T_{90} being quantized to multiples of the temporal binning (0.064 s) of the CTIME data (Meegan et al. 2009). Our measure is computed on the unbinned TTE data and thus is limited only by the 2 μs clock of the GBM DPU. A detailed study of different duration measurement techniques is warranted, but beyond the scope of this work.

In Burgess et al. (2017), we classified light curves into three classes: simple (consisting of only one significant bin), pulse like (consisting of several significant contiguous bins), and complex (consisting of non-contiguous significant bins). We will examine the parameter distributions of both the combined and individual classes below.

The selection of the Band function over the CPL was made if $2 \ln K$ of the Band function was greater than 10 that of the CPL. Here, $K = Z_{\rm Band}/Z_{\rm CPL}$. With this criterion, only 12 of the time-resolved spectra were best fit by the Band function and 513 were best fit by the CPL function. We note that the threshold of 10 is a decision made by the authors and can easily be modified. Indeed, The Band function could be used for all fits as the inability to identify a high-energy power law will result in a marginal distribution that will integrate into the other parameters naturally.

4.1 Model checking

Before assessing the parameter distribution, it is important we validate our fits to the data. Classically, GRB spectra catalogues have used various goodness-of-fit methods to quantify the validity of model fits to data. These typically involve measures of the fit maximum likelihood compared to the degrees of freedom in the model, i.e. an equivalent reduced χ^2. These measures suffer from two major statistical flaws (Andrae, Schulze-Hartung & Melchior 2010). First, reduced χ^2 measures are asymptotic. More importantly, they only apply to models linear in their parameters. Thus, it is not possible to invoke these methods to assess if the fitted model can well predict the data.

[5]The GBM mass model falls under the International Traffic in Arms Regulations (ITAR).

[6]We tested using 200, 300, and 400 live points on several simulated spectra. 400 live points are sufficient for both functions used, but we increased to 600 to have robust results.

[7]It is important to note that the use of the marginal likelihood in these settings has become increasingly scrutinized in the statistical literature (Vehtari & Ojanen 2012).

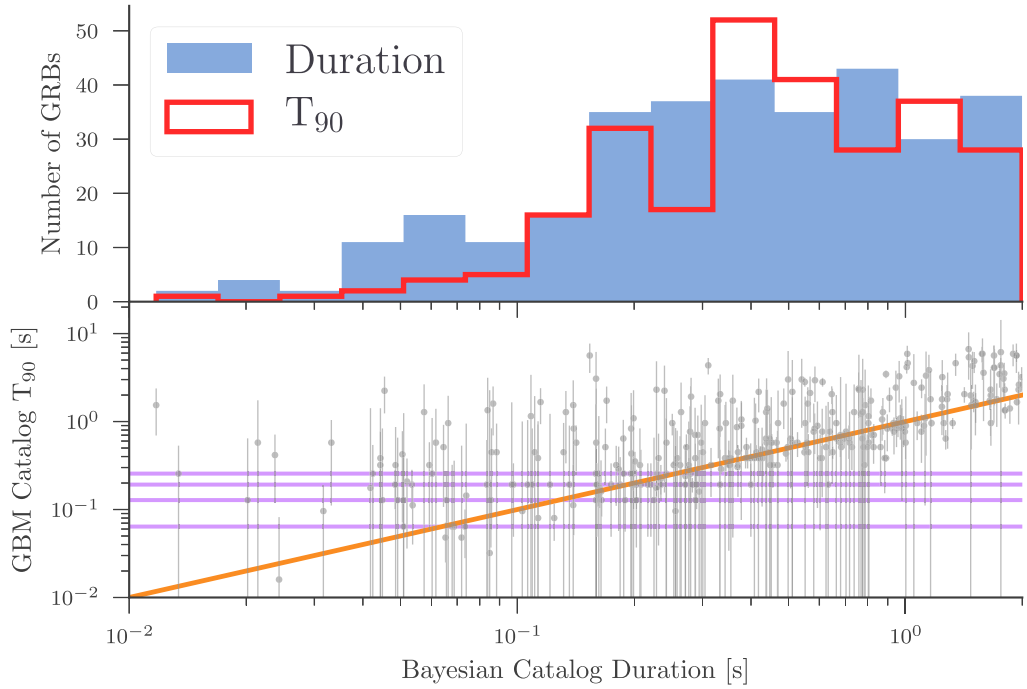

Figure 1. Top: our duration and the GBM T_{90} distributions. Bottom: comparison of the two duration measures including the errors from the GBM T_{90} measurements. The purple lines indicate four multiples of the CTIME temporal binning of 0.064 s. The orange line demonstrates a one-to-one correspondence.

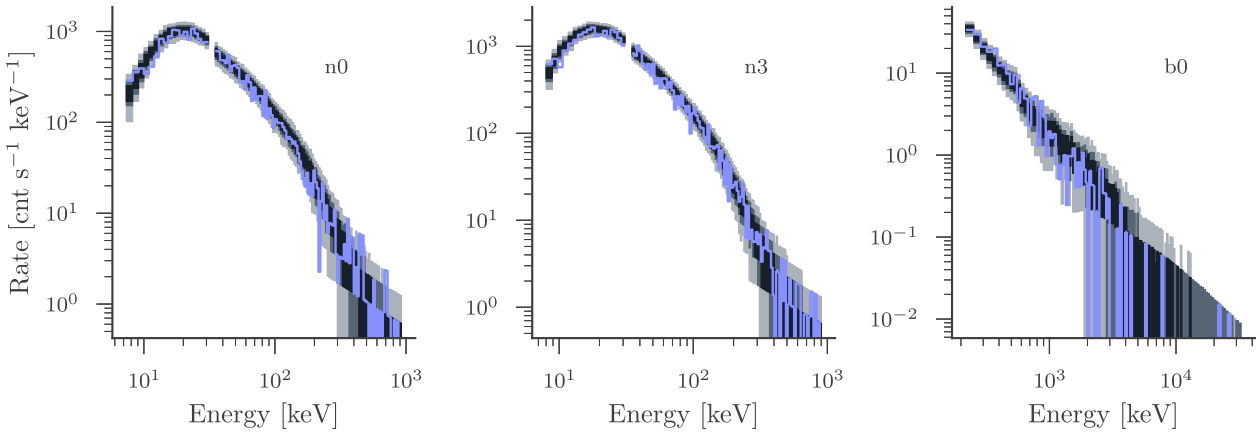

Figure 2. An example of a PPC for a spectral fit. The purple line displays the total (source+background) observed rate. The shaded regions indicate the 55th, 75th, and 95th percentile ranges of the replicated data from dark to light, respectively.

While quantitative fit assessment is preferred, when models are non-linear there are not any well-established methods that give a single number from which we can be sure that our model is working. An alternative Bayesian method is that of posterior predictive checking (PPC; Gelman 2007; Betancourt 2015, 2018). The method uses the posterior of the model fit to generate replicated data from the likelihood. Therefore, one can assess the probability of future data predicted from the model given the observed data. Mathematically,

$$\pi(y^{\rm rep}|y) = \int {\rm d}\theta\ \pi(\theta|y)\pi(y^{\rm rep}|\theta), \tag{7}$$

where θ is the posterior of the model, $y^{\rm rep}$ are replicated data, and y are the observed data.

In order to check our fits, PPCs where generated for each time interval and each detector using 500 data replications from the posterior. Both the source and background probability were taken into accounts. The procedure includes selecting a set of parameters from the posterior that defines a model spectrum. This model spectrum is then set for each detector and simulated source and background counts are generated from the likelihood. An example is displayed in Fig. 2. We note this is quite different from examining the residuals between data and model. Residual examination only investigates a single point on the posterior and data variability. Whereas PPCs integrate over both statistical processes.

Quantitatively assessing multidimensional PPCs is not a well-defined procedure. For our purposes, we examined each fit and counted the number of times the observed count rate deviated

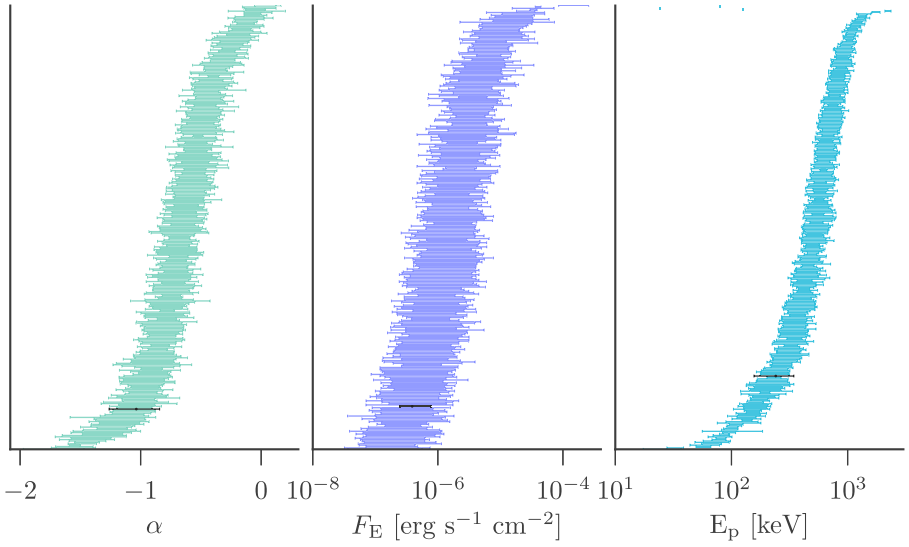

Figure 3. The distributions for α, $F_{\rm E}$, and $E_{\rm p}$, respectively. The values are plotted in increasing order along with their 68 per cent credible interval. In black, the fitted values for GRB 170817A are emphasized as they lie near the tail of the distributions for all parameters except $E_{\rm p}$.

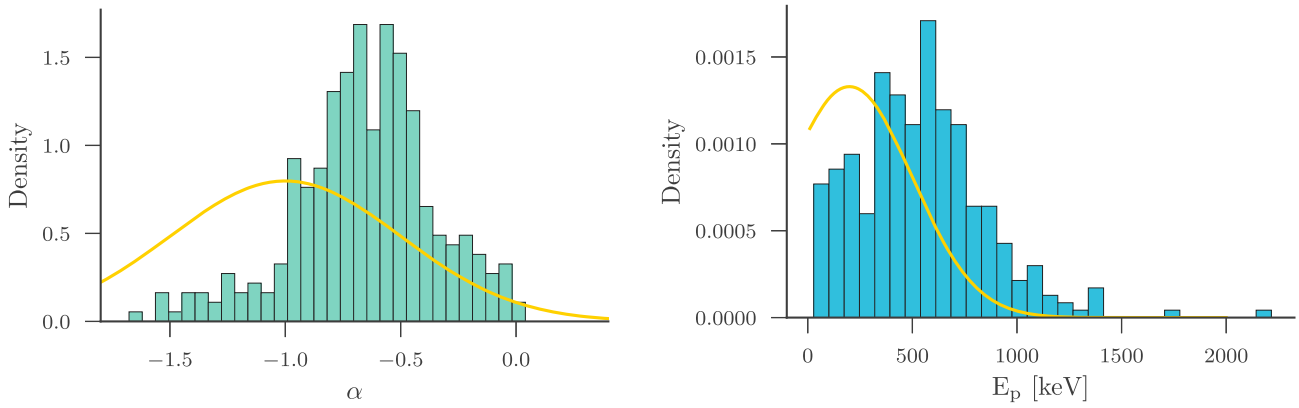

Figure 4. Histograms of parameter median values along with their priors (yellow).

from the 95th percentile predicted rates. If this occurred more than 10 times in several detectors, we considered the fit a poor representation of the data. We found that all spectral data were well modelled by the empirical functions used herein. All PPCs are include as online material.

The particularly interesting GRB 120323A (bn120323507) was modelled in the past with many different spectral components and combinations of those components (Guiriec et al. 2013). In our analysis, we have used objectively identified time intervals[8] and the proper data likelihood and our PPCs show that in most intervals of this GRB, the data are well modelled with a Band function (see online figures). The remaining intervals were well modelled with a cut-off power law. Thus, there is no need to introduce more spectral components in this analysis.

4.2 Parameter distributions

The parameter distributions[9] are displayed in Fig. 3 and are listed in Appendix A. The distributions have asymmetric tails and deviate from our assumed, weakly informative priors (see Fig. 4). This is not unexpected as our data reduction pipeline, likelihood, and general methodology differ from past approaches. This results in different measured spectra and backgrounds. Different choices of priors and interval selections will likely affect the results printed here. However, there is no motivation to analyse the use of improper likelihoods that will affect intervals with fewer source counts as the proper likelihood is known. The asymmetric tails arise from the priors influencing weaker data and thus could disappear with more sensitive measurements by future instruments.

We have additionally emphasized the parameters of GRB 170817A to demonstrate its displacement from the from the mean of the parameters. This GRB's signal is weak and its

[8]We note that in part of the analysis presented in Guiriec et al. (2013) Bayesian blocks derived from the hardness ratio of the GRB were used to identify time intervals.

[9]While we fit for the Band function's high-energy spectral index (β), we do not display these values. Of all GRBs in our sample are displayed in Fig. 3.

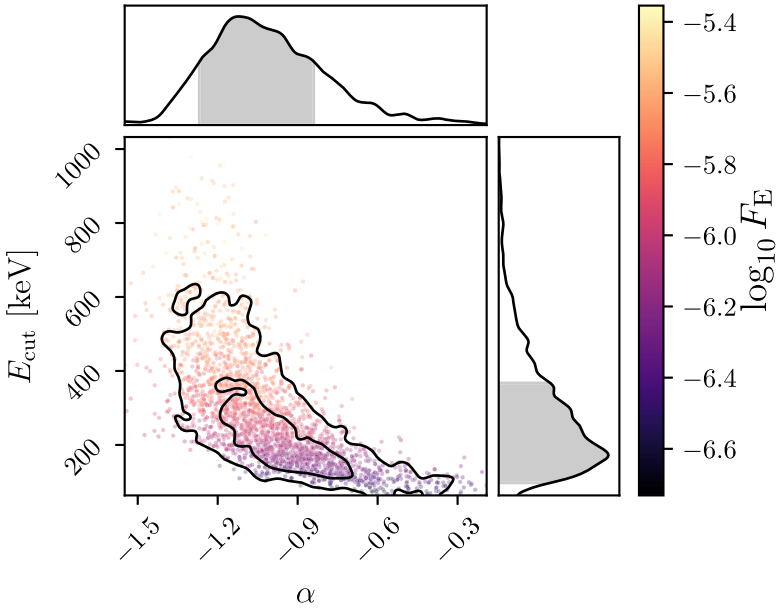

Figure 5. The conditional distributions of GRB 170817A's spectral parameters.

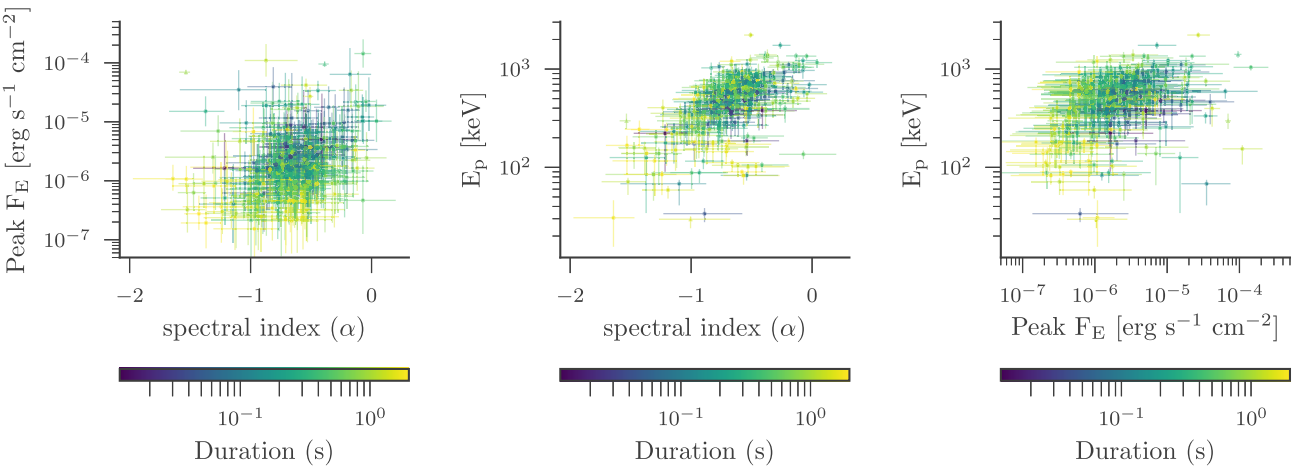

Figure 6. From left to right the α–peak $F_{\rm E}$, α–$E_{\rm p}$, and peak $F_{\rm E}$–$E_{\rm p}$ distributions from the total peak flux sample. Errors are the 0.68 credible region. The colour scale indicates the duration of the GRB. Each point represents one GRB.

parameters are more difficult to determine. This is demonstrated in Fig. 5 that displays the conditional distributions of the spectral fit.

We also examine interburst parameter correlations for both the full sample (see Fig. 6) and all light-curve structure subclasses (see Fig. 7). For each distribution, a colour scale indicating the duration of each GRB is included. Note that we combine both GRBs best modelled by the Band function and the CPL in these distributions and indicate with a triangle those parameters coming from a Band function. We do not attempt a rigorous analysis of correlations in this work because it is beyond our current scope. Such studies require proper accounting of selection effects.

5 SUMMARY

We have presented the first Bayesian *Fermi*-GBM short GRB catalogue. In the advent of the multimessenger era of astronomy, modern Bayesian methodology provides a path to rigorous and sophisticated analyses. Using the posterior distributions from our catalogue allows for non-linear error propagation of our results into further population and emission modelling studies. Compared to asymmetric errors listed previous catalogues, the propagation of these posterior samples is mathematically well founded. Our choice of priors is subjective, but mainly allows for us to incorporate our knowledge of high signal-to-noise ratio spectra into weaker spectra and enforcing our belief that spectra have a cut-off in the GBM energy range. We have checked that this does not bias our results for bright spectra where the data become more informative than the prior. Nevertheless, as detailed in the following section, we provide our spectral data so that our results can be replicated and prior choices modified as seen fit.

The models used herein are empirical and cannot be interpreted beyond their general shape. They serve to predict the data as a function of energy. Physical modelling is the only way to obtain deeper insight into the mechanisms generating the spectra. We have

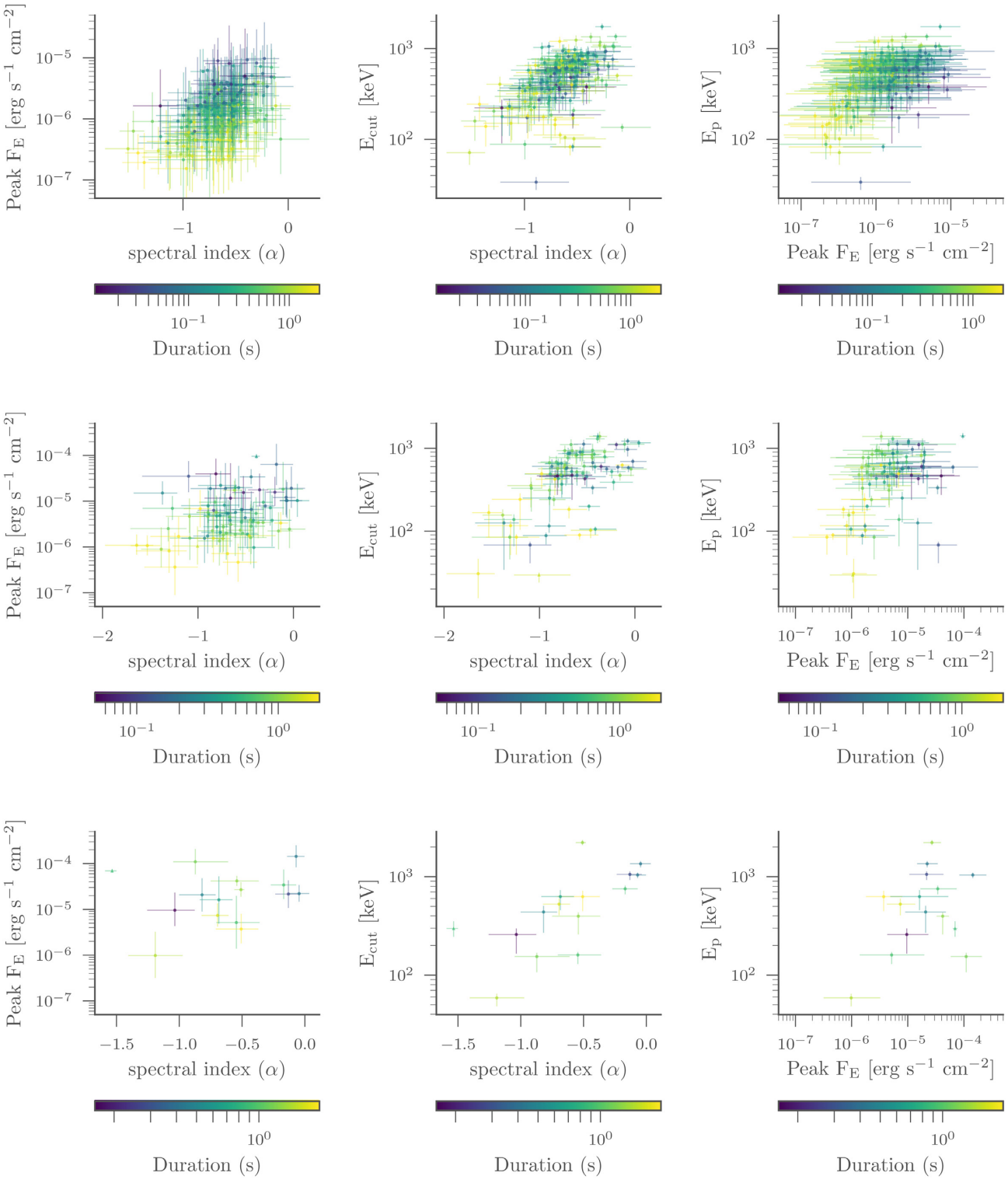

Figure 7. Same as Fig. 6, but for the simple (top), pulse-like (middle), and complex (bottom) light-curve structure subclass.

not attempted this in the current work. Thus, we caution against over interpretation of the results. Detailed physical modelling or modelling with multiple components (e.g. Guiriec et al. 2010) may indeed produce results that do not fall under the assumptions we have made. However, through our use of PPCs, we have verified that the assumptions model the data adequately.

With the confirmed association of short GRBs with a neutron star mergers, this catalogue is aimed at providing context for the observed spectral parameters of GRB 170817A. The emission possess a comparatively soft spectral slope to that of other GRBs. While we do not speculate on the physical implications of their findings, we simply note that these spectral differences may have

implications for follow-up of short GRBs in the future such as which spectral parameters are interesting. Further investigations of archival data are needed to understand the full context of this GRB.

5.1 Methodology differences

Our results differ from past catalogues and thus we find it important to detail the differences in our methodology with the past GBM catalogues. Our background fitting uses a Poisson maximum likelihood method unlike the standard GBM fitting procedure in RMFIT[10] that performs a weighted least-squares minimization with an assumption of Gaussianity of counts. As noted in Greiner et al. (2016), the method in RMFIT is improper and can lead to biased results when the number of counts in a single PHA channel is near zero. Another key difference in our analysis is the likelihood used for spectral fitting. Our use of a Poisson likelihood conditional on a Gaussian background estimate is self-consistently motivated. However, in past GBM catalogues (Goldstein et al. 2012; Gruber et al. 2014; Yu et al. 2016) and current spectral analysis (Goldstein et al. 2017), a simple Poisson likelihood is applied to the *background-subtracted* data. As demonstrated in Greiner et al. (2016), this is improper. While the total counts in GBM are Poisson distributed, background-subtracted data are not. Moreover, this is simply not the appropriate likelihood for the data.

Finally, our model selection criteria are vastly different from past catalogues. We must first disregard the improper likelihood used in past catalogues and focus on how the maximum likelihood value is applied. Typically, the ratio of these likelihoods between different spectral models is used to decide which model best fits the data. This is an invocation of Wilks' theorem (Wilks 1938). However, Wilks' theorem does not apply to non-nested or non-linear models. Therefore, simulations of the null-distribution (or null-hypothesis) must be performed to assess the confidence level at which the simpler or null-model can be rejected. This must be done for all spectral fits when the regularity conditions of Wilks' theorem are not met (Protassov et al. 2002). We have avoided this issue via the use of the marginal likelihood as a model selection tool, though we note that there is great debate in statistical literature about the use of the marginal likelihood to select models.

5.2 Data availability

To encourage replication and follow-up studies, we provide a variety of data products from this study to the community. The raw spectral and background bins are provided as PHA files readable by both 3ML and XSPEC.[11] The spectral results are included and can be read using 3ML's LOAD_ANALYSIS_RESULTS function. Additionally, we include the pre-computed F_E marginal distributions. Finally, machine readable summary tables for the time-resolved and peak flux spectral results are released.[12]

ACKNOWLEDGEMENTS

The authors gratefully acknowledge the *Fermi* GBM team's release of public data. We are additionally thankful for discussions with Daniel Mortlock. DB and FB are supported by the Deutsche Forschungsgemeinschaft (SFB 1258).

[10]https://fermi.gsfc.nasa.gov/ssc/data/analysis/rmfit/
[11]https://heasarc.gsfc.nasa.gov/xanadu/xspec/
[12]Upon publication data will be fully released. Please contact the authors for access until that time.

REFERENCES

Abbott B. P. et al., 2017a, Phys. Rev. Lett., 119, 161101
Abbott B. P. et al., 2017b, ApJ, 848, L12
Abbott B. P. et al., 2017c, ApJ, 848, L13
Andrae R., Schulze-Hartung T., Melchior P., 2010, preprint (arXiv:1012.3754)
Arnaud K., Smith R., Siemiginowska A., 2011, Handbook of X-ray Astronomy. Cambridge Univ. Press, Cambridge
Band D., Matteson J., Ford L., 1993, ApJ, 413, 281
Bartlett M. S., 1957, Biometrika, 44, 533
Bégué D., Burgess J. M., Greiner J., 2017, ApJ, 851, L19
Betancourt M., 2015, preprint (arXiv:1506.02273)
Betancourt M., 2018, preprint (arXiv:1803.08393)
Bissaldi E. et al., 2009, Exp. Astron., 24, 47
Burgess J. M., 2019, A&A, 629, A69
Burgess J. M., Ryde F., Yu H.-F., 2015, MNRAS, 451, 1511
Burgess J. M., Greiner J., Bégué D., Giannios D., Berlato F., Lipunov V. M., 2017, preprint (arXiv:1710.05823)
Burgess J. M., Yu H.-F., Greiner J., Mortlock D. J., 2018, MNRAS, 476, 1427
Chruslinska M., Belczynski K., Klencki J., Benacquista M., 2018, MNRAS, 474, 2937
Feroz F., Hobson M. P., Bridges M., 2009, MNRAS, 398, 1601
Gelman A., 2007, Int. Stat. Rev., 71, 369
Goldstein A. et al., 2012, ApJS, 199, 19
Goldstein A. et al., 2017, ApJ, 848, L14
Greiner J. et al., 1995, A&A, 302, 121
Greiner J., Burgess J. M., Savchenko V., Yu H. F., 2016, ApJ, 827, L38
Gruber D. et al., 2014, ApJS, 211, 12
Guiriec S. et al., 2010, ApJ, 725, 225
Guiriec S. et al., 2013, ApJ, 770, 32
Kasliwal M. M. et al., 2017, Science, 358, 1559
Koshut T. M., Paciesas W. S., Kouveliotou C., van Paradijs J., Pendleton G. N., Fishman G. J., Meegan C. A., 1995, BAAS, 27, 886
Li T. P., Ma Y. Q., 1983, ApJ, 272, 317
Meegan C. et al., 2009, ApJ, 702, 791
Protassov R., van Dyk D. A., Connors A., Kashyap V. L., Siemiginowska A., 2002, ApJ, 571, 545
Rowlinson A., Gompertz B. P., Dainotti M., O'Brien P. T., Wijers R. A. M. J., van der Horst A. J., 2014, MNRAS, 443, 1779
Scargle J. D., Norris J. P., Jackson B., Chiang J., 2013, ApJ, 764, 167
Strachan R. W., Dijk H. K., 2003, Oxford Bull. Economics Stat., 65, 863
Vehtari A., Ojanen J., 2012, Stat. Surv., 6, 142
Vianello G., 2018, ApJS, 236, 17
Vianello G. et al., 2015, preprint (arXiv:1507.08343)
Wilks S. S., 1938, Ann. Math. Stat., 9, 60
Yu H.-F. et al., 2016, A&A, 588, A135

SUPPORTING INFORMATION

Supplementary data are available at *MNRAS* online.

ppc.pdf

Please note: Oxford University Press is not responsible for the content or functionality of any supporting materials supplied by the authors. Any queries (other than missing material) should be directed to the corresponding author for the article.

APPENDIX A: PARAMETERS

The following table (Table A1) lists the best-fitting model and

Table A1. The best-fitting model and 68 per cent credible regions for the parameters of the spectra.

GRB	Time interval	Model	Flux (10^{-6} erg s^{-1} cm^{-2})	$E_{\rm p}$ (keV)	α
bn080723913	−0.057–0.214	CPL	$0.96^{+2.17}_{-0.65}$	$423.03^{+70.00}_{-156.23}$	$-0.79^{+0.14}_{-0.18}$
bn080725541	−0.065–0.405	CPL	$1.68^{+2.49}_{-0.88}$	$979.89^{+132.41}_{-181.69}$	$-0.63^{+0.09}_{-0.11}$
bn080802386	−0.038–0.027	CPL	$6.53^{+11.01}_{-4.03}$	$900.05^{+120.90}_{-201.56}$	$-0.55^{+0.10}_{-0.16}$
bn080802386	0.351–0.427	CPL	$3.11^{+11.56}_{-2.31}$	$485.01^{+78.03}_{-163.68}$	$-0.52^{+0.16}_{-0.24}$
bn080815917	−0.369–0.619	CPL	$0.53^{+1.16}_{-0.34}$	$382.61^{+100.95}_{-159.17}$	$-0.95^{+0.14}_{-0.19}$
bn080816989	−0.046–0.181	CPL	$3.37^{+4.16}_{-1.82}$	$1390.06^{+193.44}_{-198.50}$	$-0.37^{+0.08}_{-0.11}$
bn080816989	0.181–0.968	CPL	$2.52^{+2.83}_{-1.38}$	$1460.44^{+119.43}_{-138.10}$	$-0.15^{+0.09}_{-0.09}$
bn080828189	−0.239–0.260	CPL	$0.46^{+1.47}_{-0.33}$	$361.15^{+73.36}_{-137.47}$	$-0.90^{+0.15}_{-0.24}$
bn080831053	−0.028–0.006	CPL	$2.59^{+11.00}_{-1.97}$	$371.10^{+52.10}_{-177.17}$	$-0.67^{+0.19}_{-0.27}$
bn080905499	−0.040–0.258	CPL	$1.70^{+4.03}_{-1.20}$	$545.83^{+53.63}_{-160.86}$	$-0.47^{+0.15}_{-0.19}$
bn080919790	−0.015–0.049	CPL	$1.52^{+4.64}_{-1.10}$	$349.63^{+56.91}_{-122.20}$	$-0.76^{+0.20}_{-0.20}$
bn081012045	−0.101–0.667	CPL	$1.67^{+2.20}_{-0.95}$	$812.91^{+90.66}_{-172.76}$	$-0.53^{+0.09}_{-0.13}$
bn081024245	−0.164–0.033	CPL	$1.58^{+4.56}_{-1.19}$	$737.94^{+152.59}_{-216.54}$	$-0.66^{+0.15}_{-0.20}$
bn081024891	−0.056–0.008	CPL	$2.83^{+7.28}_{-2.14}$	$944.77^{+188.58}_{-216.96}$	$-0.44^{+0.14}_{-0.18}$
bn081024891	−0.008–0.659	CPL	$0.64^{+1.22}_{-0.41}$	$784.21^{+126.55}_{-238.46}$	$-0.72^{+0.13}_{-0.13}$
bn081101491	−0.085–0.118	CPL	$0.98^{+2.93}_{-0.68}$	$374.22^{+40.98}_{-149.67}$	$-0.77^{+0.15}_{-0.21}$
bn081105614	−0.069–0.011	CPL	$3.72^{+10.60}_{-2.69}$	$838.19^{+155.00}_{-195.23}$	$-0.33^{+0.17}_{-0.18}$
bn081113230	−0.038–0.076	CPL	$1.56^{+3.82}_{-1.05}$	$329.72^{+66.33}_{-157.41}$	$-1.09^{+0.11}_{-0.21}$
bn081113230	0.076–0.767	CPL	$0.30^{+1.78}_{-0.24}$	$338.89^{+76.66}_{-156.91}$	$-0.91^{+0.20}_{-0.30}$
bn081119184	−0.344–0.067	CPL	$0.73^{+2.42}_{-0.51}$	$574.43^{+123.62}_{-223.14}$	$-0.78^{+0.15}_{-0.21}$
bn081122614	−0.023–0.030	CPL	$2.02^{+5.03}_{-1.53}$	$173.27^{+16.00}_{-55.76}$	$-0.97^{+0.19}_{-0.22}$
bn081130212	−0.055–0.010	CPL	$0.62^{+2.29}_{-0.49}$	$33.78^{+4.73}_{-6.11}$	$-0.89^{+0.31}_{-0.34}$
bn081204517	−0.080–0.117	CPL	$1.61^{+2.51}_{-0.97}$	$431.43^{+69.23}_{-151.71}$	$-0.82^{+0.10}_{-0.16}$
bn081209981	−0.052–0.012	CPL	$18.86^{+20.93}_{-10.11}$	$605.63^{+130.72}_{-225.90}$	$-0.87^{+0.15}_{-0.21}$
bn081209981	−0.012–0.032	CPL	$3.99^{+6.69}_{-2.49}$	$970.82^{+106.88}_{-133.03}$	$-0.33^{+0.10}_{-0.10}$
bn081209981	0.032–0.168	CPL	$2.80^{+6.85}_{-2.05}$	$896.10^{+135.47}_{-184.02}$	$-0.56^{+0.10}_{-0.15}$
bn081213173	−0.029–0.014	CPL	$2.55^{+5.51}_{-1.66}$	$494.58^{+83.09}_{-187.77}$	$-0.75^{+0.13}_{-0.18}$
bn081216531	−0.135–0.013	CPL	$7.35^{+9.03}_{-3.75}$	$121.13^{+5.98}_{-37.80}$	$-0.55^{+0.37}_{-0.30}$
bn081216531	0.501–0.545	CPL	$0.53^{+1.55}_{-0.38}$	$481.41^{+61.52}_{-111.59}$	$-0.48^{+0.16}_{-0.16}$
bn081216531	0.545–0.670	CPL	$5.16^{+11.61}_{-3.35}$	$1141.87^{+81.07}_{-93.23}$	$-0.36^{+0.06}_{-0.06}$
bn081216531	0.670–0.732	CPL	$17.38^{+10.69}_{-6.29}$	$818.89^{+139.80}_{-183.67}$	$-0.62^{+0.08}_{-0.12}$
bn081216531	0.732–0.965	CPL	$0.59^{+3.05}_{-0.50}$	$221.77^{+36.76}_{-97.37}$	$-1.11^{+0.18}_{-0.23}$
bn081223419	−0.034–0.219	CPL	$1.89^{+2.15}_{-0.98}$	$199.43^{+12.16}_{-23.61}$	$-0.48^{+0.12}_{-0.11}$
bn081223419	0.219–0.419	CPL	$0.90^{+2.36}_{-0.62}$	$224.76^{+26.17}_{-83.29}$	$-0.88^{+0.15}_{-0.22}$
bn081226044	−0.193–0.139	CPL	$1.34^{+2.93}_{-0.91}$	$542.25^{+105.20}_{-156.99}$	$-0.80^{+0.15}_{-0.18}$
bn081226509	−0.069–0.148	CPL	$1.86^{+3.72}_{-1.20}$	$483.78^{+65.59}_{-110.67}$	$-0.52^{+0.12}_{-0.17}$
bn081229187	−0.060–0.219	CPL	$1.37^{+3.13}_{-0.90}$	$727.35^{+95.75}_{-218.62}$	$-0.49^{+0.14}_{-0.17}$
bn081230871	−0.233–0.546	CPL	$0.77^{+2.17}_{-0.57}$	$606.80^{+103.91}_{-187.65}$	$-0.55^{+0.15}_{-0.19}$
bn090108020	−0.140–0.044	CPL	$1.25^{+2.98}_{-0.87}$	$176.87^{+30.87}_{-96.63}$	$-1.23^{+0.15}_{-0.27}$
bn090108020	−0.044–0.146	CPL	$0.26^{+1.59}_{-0.20}$	$139.98^{+8.25}_{-8.86}$	$-0.31^{+0.13}_{-0.08}$
bn090108020	0.146–0.263	CPL	$0.61^{+2.02}_{-0.44}$	$127.82^{+9.81}_{-25.43}$	$-0.65^{+0.21}_{-0.20}$
bn090108020	0.263–0.680	CPL	$2.51^{+1.95}_{-1.19}$	$84.65^{+6.92}_{-38.94}$	$-1.31^{+0.19}_{-0.40}$
bn090108322	−0.033–0.065	CPL	$3.69^{+6.60}_{-2.36}$	$756.41^{+107.90}_{-180.83}$	$-0.54^{+0.12}_{-0.14}$

Table A1 *– continued*

GRB	Time interval	Model	Flux (10^{-6} erg s^{-1} cm^{-2})	E_p (keV)	α
bn090206620	− 0.035–0.132	CPL	$3.85^{+5.69}_{-2.21}$	$597.49^{+66.93}_{-101.33}$	$-0.42^{+0.12}_{-0.13}$
bn090206620	0.132–0.318	CPL	$0.68^{+2.34}_{-0.51}$	$441.54^{+85.41}_{-183.19}$	$-0.76^{+0.15}_{-0.23}$
bn090219074	− 0.081–0.481	CPL	$0.86^{+3.37}_{-0.65}$	$278.84^{+43.39}_{-99.65}$	$-0.94^{+0.20}_{-0.27}$
bn090225009	− 0.247–0.264	CPL	$0.89^{+2.73}_{-0.69}$	$759.77^{+170.43}_{-254.66}$	$-0.77^{+0.16}_{-0.20}$
bn090227772	− 0.019–0.010	CPL	$3.92^{+9.38}_{-2.73}$	$637.37^{+130.31}_{-180.77}$	$-0.71^{+0.14}_{-0.14}$
bn090227772	− 0.010–0.042	CPL	$0.70^{+0.97}_{-0.42}$	$1988.03^{+63.89}_{-70.40}$	$0.01^{+0.04}_{-0.04}$
bn090227772	0.042–0.134	Band	$95.56^{+11.12}_{-10.52}$	$1410.51^{+118.59}_{-110.59}$	$-0.39^{+0.03}_{-0.05}$
bn090227772	0.134–0.174	CPL	$39.13^{+12.87}_{-9.81}$	$182.15^{+17.50}_{-39.19}$	$-0.62^{+0.20}_{-0.19}$
bn090227772	0.174–0.351	CPL	$9.49^{+19.51}_{-5.95}$	$280.28^{+53.60}_{-148.31}$	$-1.29^{+0.10}_{-0.18}$
bn090228204	− 0.009–0.002	CPL	$32.14^{+35.12}_{-17.04}$	$339.60^{+58.52}_{-131.04}$	$-0.77^{+0.18}_{-0.27}$
bn090228204	− 0.002–0.019	CPL	$2.14^{+4.99}_{-1.45}$	$1061.12^{+103.05}_{-156.39}$	$-0.71^{+0.05}_{-0.08}$
bn090228204	0.019–0.034	CPL	$143.82^{+107.21}_{-60.89}$	$1040.26^{+59.76}_{-74.43}$	$-0.07^{+0.07}_{-0.07}$
bn090228204	0.034–0.081	CPL	$53.97^{+28.73}_{-20.81}$	$668.16^{+32.19}_{-32.49}$	$-0.04^{+0.06}_{-0.06}$
bn090228204	0.081–0.101	CPL	$6.17^{+20.96}_{-4.69}$	$615.99^{+43.23}_{-73.74}$	$-0.17^{+0.10}_{-0.10}$
bn090228204	0.101–0.155	CPL	$26.96^{+16.13}_{-11.22}$	$181.79^{+18.06}_{-41.81}$	$-0.76^{+0.20}_{-0.17}$
bn090228204	0.155–0.260	CPL	$0.23^{+1.54}_{-0.19}$	$57.94^{+4.85}_{-26.78}$	$-1.15^{+0.36}_{-0.42}$
bn090228204	0.260–0.433	CPL	$1.06^{+1.88}_{-0.67}$	$99.53^{+7.32}_{-15.89}$	$-0.85^{+0.19}_{-0.17}$
bn090305052	− 0.118–0.319	CPL	$1.15^{+1.82}_{-0.59}$	$759.02^{+111.77}_{-165.01}$	$-0.70^{+0.09}_{-0.12}$
bn090305052	0.319–0.792	CPL	$3.43^{+4.67}_{-1.83}$	$907.44^{+85.81}_{-129.18}$	$-0.32^{+0.10}_{-0.10}$
bn090328713	− 0.024–0.097	CPL	$6.28^{+3.69}_{-2.28}$	$1057.74^{+117.71}_{-195.22}$	$-0.77^{+0.05}_{-0.07}$
bn090331681	− 0.102–0.118	CPL	$1.46^{+2.75}_{-1.04}$	$650.55^{+113.77}_{-185.15}$	$-0.75^{+0.11}_{-0.20}$
bn090331681	0.685–0.823	CPL	$1.60^{+4.85}_{-1.19}$	$770.75^{+158.32}_{-201.97}$	$-0.45^{+0.17}_{-0.18}$
bn090405663	− 0.064–0.047	CPL	$2.55^{+5.77}_{-1.75}$	$731.41^{+110.93}_{-201.46}$	$-0.54^{+0.15}_{-0.17}$
bn090418816	− 0.107–0.025	CPL	$2.00^{+5.76}_{-1.47}$	$769.91^{+148.18}_{-183.19}$	$-0.70^{+0.14}_{-0.19}$
bn090418816	− 0.025–0.676	CPL	$0.42^{+1.51}_{-0.34}$	$703.99^{+157.41}_{-250.73}$	$-0.68^{+0.20}_{-0.21}$
bn090429753	− 0.025–0.482	CPL	$1.73^{+1.52}_{-0.74}$	$771.71^{+124.02}_{-160.28}$	$-0.83^{+0.06}_{-0.10}$
bn090510016	− 0.023–0.003	CPL	$3.28^{+6.29}_{-2.22}$	$639.56^{+123.73}_{-218.62}$	$-0.60^{+0.10}_{-0.22}$
bn090510016	0.382–0.533	CPL	$13.17^{+18.66}_{-7.36}$	$366.39^{+41.53}_{-127.52}$	$-0.50^{+0.21}_{-0.20}$
bn090510016	0.533–0.598	CPL	$26.93^{+12.12}_{-7.96}$	$2217.83^{+144.08}_{-130.32}$	$-0.51^{+0.03}_{-0.05}$
bn090510016	0.598–0.750	Band	$5.68^{+2.78}_{-2.00}$	$2402.58^{+219.83}_{-122.02}$	$-0.24^{+0.04}_{-0.06}$
bn090510016	0.750–0.823	CPL	$5.23^{+12.38}_{-3.57}$	$375.45^{+56.10}_{-137.99}$	$-0.75^{+0.13}_{-0.17}$
bn090510016	0.823–0.840	CPL	$1.32^{+4.88}_{-0.97}$	$979.59^{+147.92}_{-216.08}$	$-0.65^{+0.10}_{-0.10}$
bn090510016	0.840–1.300	CPL	$0.40^{+1.14}_{-0.30}$	$402.47^{+105.42}_{-206.54}$	$-1.09^{+0.12}_{-0.26}$
bn090518080	− 0.416–1.002	CPL	$0.42^{+0.97}_{-0.26}$	$219.70^{+36.67}_{-79.81}$	$-1.16^{+0.15}_{-0.19}$
bn090520832	− 0.443–0.138	CPL	$0.29^{+2.17}_{-0.24}$	$184.83^{+19.64}_{-87.49}$	$-0.75^{+0.32}_{-0.34}$
bn090531775	− 0.152–0.844	CPL	$1.64^{+1.88}_{-0.85}$	$1240.48^{+159.97}_{-182.35}$	$-0.51^{+0.06}_{-0.12}$
bn090610648	− 0.604–1.158	CPL	$1.08^{+1.03}_{-0.54}$	$1199.96^{+147.72}_{-187.71}$	$-0.67^{+0.07}_{-0.10}$
bn090617208	− 0.027–0.049	CPL	$12.08^{+17.09}_{-7.00}$	$968.24^{+97.71}_{-171.45}$	$-0.08^{+0.10}_{-0.14}$
bn090617208	0.049–0.133	CPL	$2.68^{+8.79}_{-2.01}$	$341.12^{+42.76}_{-105.86}$	$-0.48^{+0.18}_{-0.23}$
bn090620901	− 0.689–0.566	CPL	$0.61^{+1.62}_{-0.45}$	$667.01^{+135.91}_{-177.02}$	$-0.64^{+0.12}_{-0.22}$
bn090621922	− 0.015–0.029	CPL	$8.23^{+21.16}_{-5.78}$	$591.50^{+66.10}_{-140.33}$	$-0.30^{+0.19}_{-0.14}$
bn090802235	− 0.013–0.023	CPL	$15.43^{+19.93}_{-8.83}$	$429.87^{+45.29}_{-70.15}$	$-0.52^{+0.11}_{-0.12}$
bn090802235	0.023–0.052	CPL	$3.85^{+15.98}_{-2.94}$	$256.22^{+27.33}_{-99.51}$	$-0.82^{+0.24}_{-0.24}$
bn090814368	− 0.035–0.199	CPL	$3.56^{+4.63}_{-1.90}$	$678.35^{+58.95}_{-115.64}$	$-0.44^{+0.11}_{-0.10}$
bn090819607	− 0.121–0.063	CPL	$1.69^{+4.79}_{-1.19}$	$604.23^{+111.50}_{-193.71}$	$-0.55^{+0.14}_{-0.21}$
bn090902401	− 0.280–0.964	CPL	$1.64^{+2.42}_{-0.97}$	$503.70^{+36.45}_{-73.43}$	$-0.12^{+0.14}_{-0.11}$

Table A1 – *continued*

GRB	Time interval	Model	Flux (10^{-6} erg s^{-1} cm^{-2})	$E_{\rm p}$ (keV)	α
bn090907808	− 0.402–0.057	CPL	$0.43^{+1.52}_{-0.33}$	$346.72^{+49.21}_{-128.12}$	$-0.74^{+0.19}_{-0.22}$
bn090907808	− 0.057–0.546	CPL	$2.23^{+3.45}_{-1.34}$	$471.64^{+39.22}_{-64.95}$	$-0.16^{+0.15}_{-0.11}$
bn090909854	− 0.051–0.058	CPL	$1.70^{+4.78}_{-1.26}$	$453.50^{+110.83}_{-163.39}$	$-0.83^{+0.13}_{-0.23}$
bn090924625	− 0.051–0.150	CPL	$2.66^{+5.95}_{-1.79}$	$674.33^{+82.20}_{-167.02}$	$-0.46^{+0.13}_{-0.17}$
bn090927422	− 0.275–0.452	CPL	$0.45^{+1.03}_{-0.31}$	$246.10^{+33.56}_{-96.45}$	$-0.94^{+0.13}_{-0.23}$
bn091002685	− 0.695–0.356	CPL	$0.25^{+0.79}_{-0.18}$	$211.01^{+18.33}_{-87.29}$	$-0.94^{+0.22}_{-0.23}$
bn091006360	− 0.172–0.118	CPL	$0.57^{+2.04}_{-0.41}$	$224.90^{+33.75}_{-78.65}$	$-0.91^{+0.17}_{-0.27}$
bn091012783	− 0.066–0.019	CPL	$18.25^{+53.74}_{-13.23}$	$1119.23^{+193.57}_{-225.80}$	$-0.11^{+0.21}_{-0.17}$
bn091012783	− 0.019–0.007	CPL	$4.30^{+4.82}_{-2.36}$	$1178.96^{+128.91}_{-175.73}$	$-0.10^{+0.12}_{-0.20}$
bn091012783	0.007–0.614	CPL	$5.08^{+17.97}_{-4.03}$	$525.65^{+41.86}_{-69.98}$	$-0.38^{+0.09}_{-0.12}$
bn091017861	− 1.021–0.976	CPL	$0.28^{+0.28}_{-0.13}$	$243.73^{+55.62}_{-83.54}$	$-1.43^{+0.08}_{-0.12}$
bn091018957	− 0.101–0.107	CPL	$1.45^{+5.92}_{-1.11}$	$372.31^{+54.61}_{-104.83}$	$-0.71^{+0.21}_{-0.22}$
bn091019750	− 0.048–0.004	CPL	$1.86^{+5.38}_{-1.35}$	$318.48^{+41.22}_{-114.01}$	$-0.61^{+0.19}_{-0.21}$
bn091122163	− 0.418–0.166	CPL	$0.69^{+1.64}_{-0.50}$	$757.95^{+134.34}_{-193.76}$	$-0.69^{+0.14}_{-0.17}$
bn091126333	− 0.037–0.166	CPL	$2.52^{+4.74}_{-1.49}$	$442.59^{+45.44}_{-96.17}$	$-0.51^{+0.13}_{-0.16}$
bn091223191	− 0.221–0.307	CPL	$0.84^{+2.03}_{-0.60}$	$539.87^{+88.55}_{-166.92}$	$-0.51^{+0.18}_{-0.17}$
bn100101028	− 0.267–0.284	CPL	$0.70^{+2.15}_{-0.50}$	$686.16^{+106.20}_{-238.08}$	$-0.53^{+0.14}_{-0.20}$
bn100101988	− 1.005–0.467	CPL	$0.59^{+1.75}_{-0.43}$	$715.74^{+109.69}_{-201.30}$	$-0.31^{+0.20}_{-0.16}$
bn100107074	− 0.045–0.012	CPL	$2.77^{+13.97}_{-2.28}$	$573.89^{+118.04}_{-187.32}$	$-0.45^{+0.23}_{-0.25}$
bn100117879	− 0.077–0.165	CPL	$1.74^{+3.54}_{-1.17}$	$393.13^{+43.68}_{-97.51}$	$-0.52^{+0.19}_{-0.13}$
bn100206563	− 0.024–0.098	CPL	$7.86^{+8.82}_{-4.07}$	$562.28^{+43.27}_{-83.44}$	$-0.30^{+0.10}_{-0.10}$
bn100206563	0.098–0.139	CPL	$0.83^{+5.50}_{-0.70}$	$321.02^{+58.61}_{-160.06}$	$-0.83^{+0.27}_{-0.29}$
bn100212588	− 0.647–0.857	CPL	$0.24^{+0.61}_{-0.17}$	$150.30^{+17.23}_{-57.99}$	$-1.13^{+0.16}_{-0.26}$
bn100216422	0.010–0.184	CPL	$1.34^{+3.98}_{-0.97}$	$560.80^{+99.33}_{-165.67}$	$-0.51^{+0.20}_{-0.18}$
bn100223110	− 0.022–0.069	CPL	$0.77^{+3.63}_{-0.60}$	$322.32^{+64.10}_{-153.43}$	$-0.81^{+0.21}_{-0.29}$
bn100223110	0.069–0.208	CPL	$10.32^{+10.25}_{-5.78}$	$1220.08^{+104.00}_{-125.31}$	$-0.08^{+0.12}_{-0.07}$
bn100301068	− 0.052–0.014	CPL	$3.74^{+9.64}_{-2.61}$	$580.56^{+78.75}_{-153.36}$	$-0.55^{+0.16}_{-0.17}$
bn100326294	0.193–0.347	CPL	$2.40^{+6.69}_{-1.70}$	$922.16^{+131.98}_{-208.18}$	$-0.23^{+0.15}_{-0.18}$
bn100328141	− 0.134–0.171	CPL	$3.53^{+4.45}_{-1.88}$	$846.61^{+93.27}_{-155.38}$	$-0.43^{+0.07}_{-0.13}$
bn100328141	0.171–0.474	CPL	$1.27^{+2.18}_{-0.77}$	$620.48^{+117.19}_{-188.84}$	$-0.70^{+0.10}_{-0.15}$
bn100406758	− 0.418–1.161	CPL	$0.32^{+0.65}_{-0.23}$	$171.73^{+16.84}_{-36.37}$	$-0.54^{+0.20}_{-0.18}$
bn100411516	− 0.084–0.599	CPL	$0.45^{+1.09}_{-0.34}$	$649.05^{+137.30}_{-216.11}$	$-0.87^{+0.15}_{-0.21}$
bn100417166	− 0.026–0.023	CPL	$3.02^{+11.12}_{-2.26}$	$342.01^{+44.62}_{-104.87}$	$-0.44^{+0.20}_{-0.24}$
bn100516369	− 0.235–0.333	CPL	$0.32^{+1.42}_{-0.24}$	$228.99^{+28.60}_{-107.10}$	$-0.96^{+0.19}_{-0.29}$
bn100612545	− 0.055–0.625	CPL	$3.78^{+5.44}_{-2.21}$	$1045.41^{+94.24}_{-148.21}$	$-0.24^{+0.09}_{-0.13}$
bn100616773	− 0.319–0.081	CPL	$1.10^{+4.12}_{-0.84}$	$467.75^{+76.33}_{-168.73}$	$-0.77^{+0.11}_{-0.27}$
bn100625773	− 0.104–0.043	CPL	$5.12^{+9.31}_{-3.33}$	$555.00^{+61.57}_{-111.02}$	$-0.59^{+0.14}_{-0.13}$
bn100625773	0.084–0.167	CPL	$5.67^{+17.47}_{-4.07}$	$474.13^{+69.35}_{-119.38}$	$-0.61^{+0.16}_{-0.21}$
bn100629801	− 0.130–0.308	CPL	$2.25^{+3.11}_{-1.29}$	$240.23^{+26.65}_{-38.95}$	$-0.85^{+0.12}_{-0.15}$
bn100629801	0.308–0.768	CPL	$0.56^{+2.15}_{-0.43}$	$170.75^{+26.35}_{-66.58}$	$-1.14^{+0.25}_{-0.28}$
bn100706693	− 0.175–0.112	CPL	$1.52^{+4.12}_{-1.08}$	$847.63^{+146.22}_{-211.50}$	$-0.41^{+0.17}_{-0.16}$
bn100714686	− 0.493–0.072	CPL	$1.70^{+2.84}_{-1.04}$	$241.96^{+43.51}_{-138.24}$	$-1.20^{+0.13}_{-0.30}$
bn100714686	− 0.072–0.247	CPL	$0.27^{+0.77}_{-0.18}$	$132.68^{+7.92}_{-14.19}$	$-0.59^{+0.16}_{-0.15}$

Table A1 *– continued*

GRB	Time interval	Model	Flux (10^{-6} erg s^{-1} cm^{-2})	$E_{\rm p}$ (keV)	α
bn100714686	0.247–1.438	CPL	$0.51^{+1.63}_{-0.37}$	$39.38^{+7.85}_{-9.70}$	$-1.49^{+0.14}_{-0.35}$
bn100717446	− 0.057–0.062	CPL	$2.32^{+4.26}_{-1.48}$	$845.50^{+153.65}_{-218.99}$	$-0.56^{+0.13}_{-0.14}$
bn100717446	0.062–0.888	CPL	$0.56^{+2.02}_{-0.40}$	$432.39^{+76.13}_{-118.79}$	$-0.58^{+0.18}_{-0.19}$
bn100719311	− 0.674–0.113	CPL	$0.61^{+1.68}_{-0.43}$	$550.46^{+124.64}_{-198.99}$	$-0.63^{+0.16}_{-0.19}$
bn100719825	0.062–0.221	CPL	$0.40^{+1.54}_{-0.31}$	$231.92^{+48.47}_{-122.68}$	$-1.14^{+0.21}_{-0.29}$
bn100811108	− 0.066–0.326	CPL	$6.99^{+6.80}_{-3.16}$	$1069.24^{+93.29}_{-109.97}$	$-0.16^{+0.07}_{-0.08}$
bn100827455	− 0.067–0.008	CPL	$2.10^{+5.93}_{-1.52}$	$571.40^{+92.87}_{-181.00}$	$-0.56^{+0.14}_{-0.20}$
bn100827455	0.406–0.491	CPL	$9.48^{+9.67}_{-5.30}$	$787.99^{+71.96}_{-107.14}$	$-0.32^{+0.10}_{-0.10}$
bn100922625	− 1.237–0.524	CPL	$0.61^{+1.16}_{-0.40}$	$935.76^{+181.15}_{-200.05}$	$-0.58^{+0.11}_{-0.15}$
bn100929315	− 0.740–0.606	CPL	$0.30^{+0.44}_{-0.18}$	$404.71^{+84.39}_{-151.03}$	$-1.23^{+0.12}_{-0.13}$
bn100929916	− 0.132–0.019	CPL	$5.19^{+11.53}_{-3.41}$	$488.95^{+110.41}_{-219.53}$	$-0.89^{+0.21}_{-0.27}$
bn100929916	− 0.019–0.052	CPL	$2.82^{+5.40}_{-1.78}$	$558.54^{+81.84}_{-138.72}$	$-0.52^{+0.16}_{-0.15}$
bn100929916	0.052–0.323	CPL	$0.78^{+3.77}_{-0.64}$	$1064.18^{+162.99}_{-186.06}$	$-0.50^{+0.12}_{-0.14}$
bn101021063	− 0.173–0.614	CPL	$0.71^{+1.16}_{-0.45}$	$559.87^{+86.09}_{-182.70}$	$-0.75^{+0.12}_{-0.16}$
bn101027230	− 0.068–0.016	CPL	$1.19^{+3.51}_{-0.86}$	$418.06^{+85.54}_{-178.36}$	$-0.85^{+0.18}_{-0.21}$
bn101031625	− 0.045–0.126	CPL	$2.09^{+4.76}_{-1.34}$	$368.71^{+48.71}_{-114.14}$	$-0.77^{+0.12}_{-0.20}$
bn101031625	0.126–0.373	CPL	$0.31^{+1.43}_{-0.25}$	$190.40^{+47.89}_{-85.99}$	$-1.05^{+0.21}_{-0.34}$
bn101104810	− 0.053–0.216	CPL	$2.45^{+4.23}_{-1.51}$	$561.30^{+43.64}_{-99.65}$	$-0.04^{+0.17}_{-0.10}$
bn101104810	0.216–0.822	CPL	$1.32^{+2.68}_{-0.80}$	$823.88^{+115.29}_{-151.16}$	$-0.37^{+0.15}_{-0.13}$
bn101116481	− 0.063–0.001	CPL	$2.00^{+7.14}_{-1.57}$	$484.01^{+93.20}_{-144.07}$	$-0.53^{+0.19}_{-0.23}$
bn101129652	− 0.077–0.345	CPL	$4.77^{+5.50}_{-2.57}$	$1360.50^{+100.22}_{-129.61}$	$-0.13^{+0.10}_{-0.08}$
bn101129726	0.023–0.086	CPL	$5.72^{+7.55}_{-3.14}$	$567.30^{+120.10}_{-222.63}$	$-0.81^{+0.15}_{-0.21}$
bn101129726	0.086–0.546	CPL	$2.27^{+2.91}_{-1.19}$	$751.73^{+97.41}_{-179.24}$	$-0.64^{+0.09}_{-0.11}$
bn101204343	− 0.019–0.066	CPL	$4.00^{+6.43}_{-2.29}$	$817.24^{+174.79}_{-177.13}$	$-0.58^{+0.10}_{-0.14}$
bn101208203	− 0.253–0.379	CPL	$0.50^{+1.76}_{-0.36}$	$419.84^{+70.06}_{-157.08}$	$-0.61^{+0.17}_{-0.22}$
bn101214748	− 0.033–0.020	CPL	$4.34^{+14.71}_{-3.30}$	$454.66^{+80.80}_{-114.83}$	$-0.51^{+0.20}_{-0.18}$
bn101214748	0.020–0.207	CPL	$0.30^{+1.42}_{-0.23}$	$192.46^{+39.75}_{-120.55}$	$-1.23^{+0.20}_{-0.30}$
bn101224227	− 0.063–0.296	CPL	$0.72^{+1.53}_{-0.46}$	$388.79^{+74.59}_{-151.86}$	$-1.01^{+0.11}_{-0.19}$
bn110112934	− 0.059–0.169	CPL	$1.60^{+2.44}_{-0.96}$	$565.41^{+103.62}_{-153.23}$	$-0.75^{+0.10}_{-0.15}$
bn110131780	− 0.256–0.152	CPL	$0.62^{+1.73}_{-0.44}$	$548.76^{+99.85}_{-204.52}$	$-0.68^{+0.16}_{-0.21}$
bn110209165	− 3.945–2.013	CPL	$0.46^{+1.34}_{-0.33}$	$619.48^{+92.64}_{-223.07}$	$-0.67^{+0.13}_{-0.20}$
bn110212550	− 0.055–0.015	CPL	$1.69^{+4.60}_{-1.17}$	$441.34^{+89.76}_{-191.50}$	$-0.92^{+0.14}_{-0.21}$
bn110212550	− 0.015–0.018	CPL	$17.67^{+22.29}_{-9.86}$	$603.15^{+51.71}_{-88.24}$	$-0.35^{+0.09}_{-0.12}$
bn110227009	− 0.205–0.610	CPL	$0.55^{+2.08}_{-0.41}$	$373.61^{+55.76}_{-125.65}$	$-0.38^{+0.24}_{-0.20}$
bn110307972	− 0.054–0.705	CPL	$0.89^{+2.26}_{-0.62}$	$643.03^{+110.50}_{-170.07}$	$-0.57^{+0.10}_{-0.22}$
bn110331604	− 0.554–1.438	CPL	$0.89^{+1.63}_{-0.55}$	$771.54^{+93.03}_{-153.74}$	$-0.45^{+0.10}_{-0.15}$
bn110401920	− 0.085–0.095	CPL	$4.54^{+5.37}_{-2.42}$	$1108.23^{+171.10}_{-208.75}$	$-0.67^{+0.07}_{-0.12}$
bn110401920	0.380–0.673	CPL	$2.10^{+4.53}_{-1.44}$	$714.81^{+106.59}_{-180.54}$	$-0.60^{+0.14}_{-0.17}$
bn110409179	− 0.014–0.052	CPL	$4.95^{+9.35}_{-3.26}$	$671.09^{+79.83}_{-171.84}$	$-0.42^{+0.14}_{-0.16}$
bn110420946	− 0.018–0.002	CPL	$8.09^{+25.78}_{-6.05}$	$480.69^{+57.66}_{-159.02}$	$-0.56^{+0.17}_{-0.23}$
bn110422029	− 0.055–0.011	CPL	$1.89^{+5.42}_{-1.29}$	$579.90^{+118.42}_{-203.64}$	$-0.79^{+0.14}_{-0.18}$
bn110509475	− 0.179–0.268	CPL	$0.97^{+1.32}_{-0.53}$	$414.33^{+72.42}_{-147.93}$	$-0.95^{+0.09}_{-0.15}$
bn110511616	− 2.281–0.387	CPL	$0.19^{+0.39}_{-0.12}$	$138.79^{+20.01}_{-55.58}$	$-1.37^{+0.12}_{-0.21}$

Table A1 – *continued*

GRB	Time interval	Model	Flux (10^{-6} erg s^{-1} cm^{-2})	$E_{\rm p}$ (keV)	α
bn110517453	−0.047–0.113	CPL	$1.17^{+2.88}_{-0.81}$	$542.85^{+89.68}_{-165.20}$	$-0.71^{+0.14}_{-0.19}$
bn110526715	−0.064–0.485	CPL	$2.24^{+2.02}_{-0.96}$	$583.40^{+61.11}_{-116.55}$	$-0.78^{+0.08}_{-0.09}$
bn110529034	−0.074–0.000	CPL	$9.27^{+11.54}_{-4.81}$	$344.59^{+41.69}_{-141.58}$	$-0.58^{+0.27}_{-0.21}$
bn110529034	−0.000–0.032	CPL	$2.05^{+2.27}_{-0.99}$	$1334.64^{+183.89}_{-190.98}$	$-0.68^{+0.07}_{-0.08}$
bn110529034	0.032–0.069	CPL	$11.89^{+10.43}_{-5.23}$	$1270.26^{+129.31}_{-200.59}$	$-0.78^{+0.05}_{-0.06}$
bn110529034	0.069–0.108	CPL	$19.88^{+11.31}_{-6.04}$	$834.87^{+120.56}_{-183.57}$	$-0.61^{+0.09}_{-0.11}$
bn110529034	0.108–0.479	CPL	$1.21^{+5.13}_{-0.96}$	$528.41^{+74.44}_{-109.98}$	$-0.79^{+0.07}_{-0.11}$
bn110605780	−0.414–1.064	CPL	$0.45^{+1.13}_{-0.30}$	$321.33^{+56.48}_{-108.15}$	$-0.88^{+0.13}_{-0.20}$
bn110624906	−1.297–0.500	CPL	$0.15^{+0.67}_{-0.12}$	$181.16^{+20.23}_{-79.00}$	$-0.97^{+0.20}_{-0.34}$
bn110705151	−0.077–0.007	CPL	$11.65^{+15.87}_{-6.76}$	$678.24^{+133.63}_{-248.32}$	$-0.60^{+0.16}_{-0.22}$
bn110705151	−0.007–0.084	CPL	$19.12^{+21.40}_{-10.30}$	$1067.48^{+91.02}_{-115.99}$	$-0.19^{+0.07}_{-0.10}$
bn110705151	0.084–0.142	CPL	$1.77^{+5.36}_{-1.32}$	$807.67^{+83.66}_{-134.34}$	$-0.25^{+0.11}_{-0.12}$
bn110705151	0.142–0.206	CPL	$21.66^{+21.51}_{-10.99}$	$1055.98^{+77.84}_{-128.46}$	$-0.13^{+0.09}_{-0.10}$
bn110717180	−0.012–0.041	CPL	$9.27^{+15.69}_{-5.61}$	$519.65^{+49.23}_{-97.36}$	$-0.39^{+0.14}_{-0.12}$
bn110728056	−0.111–0.717	CPL	$0.80^{+1.68}_{-0.54}$	$738.71^{+123.49}_{-171.41}$	$-0.51^{+0.13}_{-0.15}$
bn110801335	−0.137–0.466	CPL	$0.91^{+1.83}_{-0.59}$	$204.52^{+34.68}_{-76.79}$	$-1.29^{+0.14}_{-0.19}$
bn110916016	−0.883–0.277	CPL	$0.43^{+1.41}_{-0.33}$	$341.28^{+43.00}_{-90.03}$	$-0.45^{+0.22}_{-0.21}$
bn111001804	−0.125–0.230	CPL	$0.78^{+2.23}_{-0.58}$	$569.80^{+113.78}_{-188.38}$	$-0.62^{+0.17}_{-0.20}$
bn111011094	−0.035–0.136	CPL	$3.02^{+4.28}_{-1.62}$	$420.79^{+47.14}_{-99.03}$	$-0.66^{+0.10}_{-0.15}$
bn111022854	−0.036–0.100	CPL	$1.56^{+3.99}_{-1.05}$	$428.07^{+64.93}_{-135.83}$	$-0.78^{+0.14}_{-0.19}$
bn111024896	−0.051–0.254	CPL	$0.75^{+2.62}_{-0.54}$	$403.82^{+70.87}_{-154.44}$	$-0.65^{+0.18}_{-0.22}$
bn111103948	−0.031–0.000	CPL	$3.83^{+10.47}_{-2.84}$	$524.13^{+77.10}_{-152.17}$	$-0.66^{+0.13}_{-0.23}$
bn111103948	−0.000–0.339	CPL	$2.04^{+3.53}_{-1.21}$	$999.70^{+142.78}_{-166.74}$	$-0.44^{+0.10}_{-0.14}$
bn111112908	−0.033–0.117	CPL	$5.41^{+5.10}_{-2.32}$	$869.63^{+103.13}_{-141.69}$	$-0.68^{+0.08}_{-0.08}$
bn111112908	0.117–0.202	CPL	$1.39^{+4.47}_{-0.97}$	$269.28^{+40.39}_{-103.72}$	$-0.85^{+0.16}_{-0.23}$
bn111117510	−0.083–0.130	CPL	$1.77^{+3.77}_{-1.13}$	$727.38^{+130.99}_{-183.70}$	$-0.63^{+0.10}_{-0.18}$
bn111117510	0.344–0.409	CPL	$3.82^{+9.67}_{-2.81}$	$389.72^{+38.39}_{-77.19}$	$-0.22^{+0.20}_{-0.14}$
bn111222619	−0.011–0.021	CPL	$19.28^{+15.00}_{-9.06}$	$479.97^{+57.57}_{-83.96}$	$-0.79^{+0.10}_{-0.10}$
bn111222619	0.021–0.277	CPL	$3.38^{+12.48}_{-2.53}$	$731.23^{+37.67}_{-56.99}$	$-0.24^{+0.08}_{-0.07}$
bn111222619	0.277–0.324	CPL	$22.13^{+23.69}_{-11.28}$	$461.69^{+83.92}_{-185.21}$	$-0.76^{+0.17}_{-0.24}$
bn120101354	−0.085–0.105	CPL	$0.96^{+3.17}_{-0.72}$	$267.17^{+27.71}_{-87.36}$	$-0.56^{+0.21}_{-0.22}$
bn120210650	−0.096–0.358	CPL	$0.41^{+0.29}_{-0.17}$	$280.55^{+38.75}_{-77.99}$	$-1.34^{+0.07}_{-0.09}$
bn120210650	0.358–0.819	CPL	$0.18^{+0.28}_{-0.11}$	$108.62^{+29.43}_{-52.89}$	$-1.77^{+0.06}_{-0.11}$
bn120210650	0.819–1.710	CPL	$1.07^{+0.72}_{-0.42}$	$167.11^{+42.44}_{-83.28}$	$-1.53^{+0.14}_{-0.17}$
bn120212353	−0.185–0.182	CPL	$0.85^{+3.20}_{-0.65}$	$613.42^{+86.77}_{-205.86}$	$-0.56^{+0.18}_{-0.23}$
bn120302722	−0.084–0.402	CPL	$0.49^{+2.25}_{-0.39}$	$208.10^{+19.13}_{-63.60}$	$-0.53^{+0.30}_{-0.26}$
bn120314412	−0.445–0.203	CPL	$0.43^{+1.64}_{-0.33}$	$357.91^{+45.19}_{-137.91}$	$-0.72^{+0.20}_{-0.24}$
bn120323507	−0.017–0.010	CPL	$12.85^{+2.22}_{-1.74}$	$588.31^{+124.21}_{-224.13}$	$-0.80^{+0.15}_{-0.19}$
bn120323507	−0.010–0.001	CPL	$7.90^{+1.60}_{-1.28}$	$386.26^{+41.94}_{-87.96}$	$-0.69^{+0.12}_{-0.13}$
bn120323507	0.001–0.022	Band	$64.29^{+24.46}_{-18.49}$	$123.04^{+8.82}_{-11.37}$	$-0.21^{+0.14}_{-0.12}$
bn120323507	0.022–0.094	Band	$30.24^{+24.52}_{-12.60}$	$58.91^{+1.47}_{-2.43}$	$-0.20^{+0.09}_{-0.05}$
bn120323507	0.094–0.122	Band	$9.69^{+2.92}_{-2.28}$	$399.84^{+40.73}_{-47.56}$	$-1.46^{+0.03}_{-0.03}$
bn120323507	0.122–0.148	Band	$69.52^{+6.81}_{-6.16}$	$297.43^{+54.58}_{-51.64}$	$-1.53^{+0.03}_{-0.06}$
bn120323507	0.148–0.200	Band	$3.44^{+3.13}_{-1.30}$	$167.43^{+16.73}_{-27.95}$	$-1.56^{+0.05}_{-0.06}$
bn120323507	0.200–0.252	Band	$5.61^{+3.08}_{-1.75}$	$107.85^{+11.38}_{-19.29}$	$-1.45^{+0.08}_{-0.10}$

Table A1 *– continued*

GRB	Time interval	Model	Flux (10^{-6} erg s^{-1} cm^{-2})	$E_{\rm p}$ (keV)	α
bn120323507	0.252–0.391	Band	$16.42^{+2.79}_{-2.38}$	$50.25^{+6.71}_{-6.62}$	$-1.53^{+0.07}_{-0.18}$
bn120323507	0.391–0.447	Band	$34.26^{+4.33}_{-4.05}$	$-29.75^{+52.71}_{-15.48}$	$-1.99^{+0.05}_{-0.23}$
bn120323507	0.447–0.581	Band	$64.16^{+14.15}_{-11.98}$	$-15.95^{+41.08}_{-7.75}$	$-1.91^{+0.07}_{-0.33}$
bn120323507	0.581–0.874	CPL	$0.30^{+0.42}_{-0.16}$	$18.97^{+2.08}_{-4.86}$	$-1.37^{+0.09}_{-0.26}$
bn120327418	− 0.093–0.067	CPL	$1.40^{+4.29}_{-1.06}$	$357.58^{+67.33}_{-145.81}$	$-0.73^{+0.17}_{-0.24}$
bn120403857	− 1.427–0.061	CPL	$0.24^{+0.91}_{-0.18}$	$316.77^{+48.72}_{-138.15}$	$-0.91^{+0.14}_{-0.27}$
bn120410585	− 0.072–0.127	CPL	$2.56^{+5.10}_{-1.71}$	$654.81^{+51.04}_{-139.77}$	$-0.30^{+0.17}_{-0.12}$
bn120415891	− 0.197–0.053	CPL	$1.24^{+2.55}_{-0.79}$	$682.44^{+128.84}_{-176.22}$	$-0.70^{+0.13}_{-0.15}$
bn120429003	− 0.345–1.170	CPL	$0.36^{+0.70}_{-0.21}$	$260.19^{+37.64}_{-89.52}$	$-0.99^{+0.12}_{-0.19}$
bn120519721	− 0.060–0.009	CPL	$3.52^{+15.16}_{-2.81}$	$673.88^{+89.01}_{-193.59}$	$-0.34^{+0.18}_{-0.25}$
bn120519721	0.201–0.810	CPL	$3.91^{+4.58}_{-1.85}$	$831.58^{+76.34}_{-129.78}$	$-0.45^{+0.08}_{-0.11}$
bn120524134	− 0.045–0.046	CPL	$1.55^{+4.39}_{-1.10}$	$88.33^{+7.87}_{-19.14}$	$-0.93^{+0.22}_{-0.24}$
bn120524134	0.046–0.247	CPL	$0.41^{+1.38}_{-0.30}$	$47.11^{+5.24}_{-17.40}$	$-1.30^{+0.23}_{-0.33}$
bn120603439	− 0.037–0.194	CPL	$3.70^{+5.75}_{-2.17}$	$713.05^{+106.72}_{-137.21}$	$-0.52^{+0.10}_{-0.13}$
bn120608489	− 0.054–0.147	CPL	$1.89^{+4.25}_{-1.25}$	$518.40^{+65.30}_{-126.10}$	$-0.61^{+0.14}_{-0.18}$
bn120608489	0.571–0.748	CPL	$0.80^{+3.05}_{-0.63}$	$311.64^{+38.38}_{-129.18}$	$-0.82^{+0.19}_{-0.28}$
bn120609580	− 0.318–0.962	CPL	$0.33^{+0.76}_{-0.24}$	$101.04^{+6.43}_{-18.02}$	$-0.53^{+0.30}_{-0.13}$
bn120612687	− 0.160–0.028	CPL	$3.63^{+6.32}_{-2.12}$	$826.66^{+121.85}_{-190.78}$	$-0.45^{+0.13}_{-0.13}$
bn120616630	− 0.033–0.039	CPL	$4.85^{+12.17}_{-3.43}$	$761.64^{+108.82}_{-177.27}$	$-0.16^{+0.18}_{-0.14}$
bn120619884	− 0.155–0.397	CPL	$1.14^{+3.14}_{-0.81}$	$649.72^{+67.25}_{-145.91}$	$-0.21^{+0.15}_{-0.18}$
bn120624309	− 0.034–0.007	CPL	$5.70^{+17.12}_{-4.11}$	$802.74^{+153.27}_{-236.76}$	$-0.78^{+0.11}_{-0.17}$
bn120624309	0.007–0.037	CPL	$1.03^{+2.74}_{-0.71}$	$1286.09^{+149.76}_{-211.23}$	$-0.71^{+0.06}_{-0.07}$
bn120624309	0.037–0.087	CPL	$32.89^{+10.57}_{-8.64}$	$2760.34^{+160.64}_{-162.37}$	$-0.69^{+0.03}_{-0.04}$
bn120624309	0.087–0.156	CPL	$19.51^{+7.83}_{-5.05}$	$2600.62^{+155.10}_{-155.35}$	$-0.58^{+0.03}_{-0.04}$
bn120624309	0.156–0.268	CPL	$19.37^{+15.56}_{-7.99}$	$2103.46^{+157.79}_{-159.92}$	$-0.59^{+0.03}_{-0.05}$
bn120624309	0.268–0.310	CPL	$41.85^{+12.17}_{-9.21}$	$396.97^{+35.95}_{-138.16}$	$-0.54^{+0.17}_{-0.21}$
bn120624309	0.310–0.564	CPL	$0.26^{+0.87}_{-0.19}$	$273.78^{+40.24}_{-107.76}$	$-0.96^{+0.15}_{-0.22}$
bn120624309	0.564–1.228	CPL	$0.05^{+2.14}_{-0.05}$	$184.27^{+36.36}_{-102.33}$	$-1.24^{+0.15}_{-0.28}$
bn120624309	1.228–1.235	CPL	$4.41^{+7.72}_{-2.87}$	$276.09^{+53.41}_{-262.96}$	$-1.09^{+0.42}_{-0.40}$
bn120811014	− 0.013–0.155	CPL	$10.27^{+13.59}_{-5.74}$	$1162.97^{+97.36}_{-129.51}$	$0.04^{+0.12}_{-0.09}$
bn120811014	0.236–0.357	CPL	$5.44^{+6.61}_{-2.91}$	$1236.95^{+164.81}_{-170.83}$	$-0.51^{+0.08}_{-0.11}$
bn120814201	− 0.324–0.678	CPL	$1.68^{+2.90}_{-1.03}$	$710.49^{+82.95}_{-165.71}$	$-0.66^{+0.09}_{-0.16}$
bn120822628	0.004–0.016	CPL	$1.63^{+4.79}_{-1.19}$	$221.99^{+51.95}_{-131.92}$	$-1.22^{+0.18}_{-0.26}$
bn120830297	− 0.065–0.891	CPL	$4.02^{+2.94}_{-1.82}$	$1089.96^{+86.15}_{-108.45}$	$-0.28^{+0.07}_{-0.07}$
bn120831901	− 0.061–0.052	CPL	$3.52^{+6.06}_{-2.21}$	$711.94^{+131.69}_{-191.61}$	$-0.57^{+0.11}_{-0.16}$
bn120915000	− 0.164–0.347	CPL	$1.43^{+3.12}_{-0.97}$	$732.92^{+131.85}_{-220.36}$	$-0.40^{+0.13}_{-0.18}$
bn120916085	− 0.279–0.015	CPL	$1.22^{+3.65}_{-0.88}$	$894.60^{+168.74}_{-228.42}$	$-0.40^{+0.16}_{-0.20}$
bn121004211	− 0.299–1.218	CPL	$0.34^{+1.09}_{-0.25}$	$176.28^{+14.82}_{-63.35}$	$-0.82^{+0.19}_{-0.24}$
bn121008424	− 0.282–0.609	CPL	$0.55^{+0.94}_{-0.32}$	$367.95^{+61.61}_{-137.26}$	$-0.97^{+0.09}_{-0.18}$
bn121012724	− 0.112–0.300	CPL	$2.48^{+3.44}_{-1.31}$	$546.04^{+61.43}_{-113.54}$	$-0.50^{+0.10}_{-0.12}$
bn121014638	− 0.483–0.186	CPL	$0.75^{+1.44}_{-0.51}$	$577.94^{+134.04}_{-167.37}$	$-0.96^{+0.14}_{-0.17}$
bn121023322	− 0.068–0.391	CPL	$2.75^{+2.36}_{-1.25}$	$936.28^{+141.92}_{-169.89}$	$-0.73^{+0.06}_{-0.09}$
bn121023322	0.391–0.760	CPL	$0.56^{+1.46}_{-0.41}$	$519.83^{+141.04}_{-216.66}$	$-1.00^{+0.14}_{-0.21}$
bn121102064	0.243–0.576	CPL	$1.16^{+3.94}_{-0.88}$	$769.76^{+130.20}_{-212.08}$	$-0.62^{+0.17}_{-0.18}$

Table A1 – *continued*

GRB	Time interval	Model	Flux (10^{-6} erg s^{-1} cm^{-2})	$E_{\rm p}$ (keV)	α
bn121112806	−0.201–0.537	CPL	$0.96^{+2.14}_{-0.67}$	$1174.17^{+192.55}_{-215.68}$	$-0.28^{+0.17}_{-0.14}$
bn121116459	−0.714–0.265	CPL	$0.91^{+4.16}_{-0.72}$	$452.11^{+58.44}_{-134.93}$	$-0.32^{+0.18}_{-0.24}$
bn121119579	−0.217–0.237	CPL	$0.71^{+1.46}_{-0.47}$	$183.20^{+17.09}_{-40.61}$	$-0.69^{+0.19}_{-0.17}$
bn121119579	0.237–1.584	CPL	$0.28^{+0.73}_{-0.21}$	$89.52^{+6.93}_{-23.88}$	$-1.07^{+0.24}_{-0.24}$
bn121124606	−0.042–0.041	CPL	$11.63^{+55.79}_{-9.65}$	$473.67^{+121.23}_{-235.15}$	$-0.66^{+0.21}_{-0.27}$
bn121124606	−0.041–0.019	CPL	$2.22^{+6.17}_{-1.52}$	$615.68^{+111.49}_{-211.61}$	$-0.59^{+0.14}_{-0.21}$
bn121127914	−0.017–0.171	CPL	$7.38^{+7.99}_{-3.71}$	$973.50^{+99.00}_{-138.51}$	$-0.52^{+0.07}_{-0.11}$
bn121211574	−0.695–0.996	CPL	$0.22^{+0.75}_{-0.16}$	$144.64^{+14.86}_{-36.43}$	$-0.71^{+0.23}_{-0.25}$
bn130112353	−0.316–0.303	CPL	$0.74^{+1.37}_{-0.51}$	$560.31^{+84.09}_{-194.33}$	$-0.72^{+0.14}_{-0.16}$
bn130112353	0.303–0.969	CPL	$1.51^{+1.61}_{-0.78}$	$587.68^{+68.06}_{-127.67}$	$-0.74^{+0.08}_{-0.11}$
bn130127743	−0.020–0.054	CPL	$5.53^{+10.42}_{-3.80}$	$761.90^{+79.32}_{-159.83}$	$-0.24^{+0.13}_{-0.17}$
bn130204484	−0.016–0.023	CPL	$5.97^{+8.03}_{-3.36}$	$698.03^{+112.66}_{-164.02}$	$-0.81^{+0.10}_{-0.12}$
bn130219626	−0.076–0.064	CPL	$1.47^{+4.59}_{-1.07}$	$383.18^{+51.71}_{-106.73}$	$-0.53^{+0.20}_{-0.17}$
bn130307126	−0.039–0.027	CPL	$5.47^{+6.39}_{-2.82}$	$861.09^{+149.47}_{-158.67}$	$-0.70^{+0.09}_{-0.11}$
bn130307126	0.027–0.312	CPL	$3.78^{+2.98}_{-1.72}$	$1239.29^{+174.43}_{-191.41}$	$-0.61^{+0.06}_{-0.09}$
bn130416770	−0.007–0.002	CPL	$9.10^{+23.52}_{-6.47}$	$497.17^{+85.08}_{-187.68}$	$-0.64^{+0.19}_{-0.16}$
bn130416770	0.027–0.077	CPL	$15.70^{+18.40}_{-7.81}$	$1104.59^{+85.61}_{-128.32}$	$-0.19^{+0.10}_{-0.09}$
bn130504314	−0.019–0.076	CPL	$22.15^{+12.02}_{-7.46}$	$1352.08^{+89.66}_{-109.15}$	$-0.05^{+0.08}_{-0.08}$
bn130504314	0.076–0.191	CPL	$3.37^{+9.18}_{-2.21}$	$841.76^{+137.94}_{-148.34}$	$-0.62^{+0.10}_{-0.12}$
bn130504314	0.191–0.366	CPL	$15.74^{+16.66}_{-7.69}$	$1230.07^{+66.08}_{-81.19}$	$-0.29^{+0.05}_{-0.06}$
bn130504314	0.366–0.409	CPL	$4.59^{+7.42}_{-2.60}$	$417.01^{+65.86}_{-152.54}$	$-0.81^{+0.14}_{-0.20}$
bn130515056	−0.039–0.035	CPL	$10.27^{+15.99}_{-6.05}$	$582.06^{+38.18}_{-66.92}$	$-0.07^{+0.16}_{-0.08}$
bn130515056	0.035–0.160	CPL	$2.31^{+7.67}_{-1.89}$	$250.33^{+23.22}_{-60.86}$	$-0.48^{+0.24}_{-0.24}$
bn130518551	−0.018–0.165	CPL	$2.47^{+5.09}_{-1.57}$	$1443.97^{+165.36}_{-179.23}$	$-0.48^{+0.07}_{-0.07}$
bn130518551	0.165–0.399	CPL	$1.15^{+1.46}_{-0.62}$	$669.56^{+111.49}_{-196.07}$	$-0.56^{+0.11}_{-0.17}$
bn130518551	0.399–1.677	CPL	$7.37^{+6.23}_{-3.14}$	$526.19^{+71.42}_{-121.72}$	$-0.69^{+0.09}_{-0.13}$
bn130617564	−0.501–0.109	CPL	$1.50^{+3.21}_{-1.01}$	$522.46^{+80.34}_{-150.47}$	$-0.74^{+0.15}_{-0.18}$
bn130622615	−1.058–0.602	CPL	$0.30^{+0.65}_{-0.22}$	$164.45^{+13.98}_{-37.70}$	$-0.71^{+0.17}_{-0.23}$
bn130626452	−0.057–0.113	CPL	$1.14^{+4.61}_{-0.86}$	$344.18^{+58.10}_{-138.27}$	$-0.99^{+0.17}_{-0.26}$
bn130628860	−0.010–0.033	CPL	$1.85^{+5.97}_{-1.36}$	$1042.44^{+89.11}_{-135.50}$	$-0.16^{+0.09}_{-0.13}$
bn130628860	0.033–0.092	CPL	$1.64^{+3.51}_{-1.04}$	$410.62^{+87.74}_{-137.38}$	$-0.82^{+0.15}_{-0.22}$
bn130628860	0.352–0.488	CPL	$20.80^{+26.95}_{-11.80}$	$437.85^{+67.72}_{-168.66}$	$-0.82^{+0.11}_{-0.18}$
bn130705398	−0.045–0.180	CPL	$1.33^{+3.35}_{-0.97}$	$722.37^{+125.62}_{-186.69}$	$-0.52^{+0.16}_{-0.19}$
bn130706900	−0.038–0.013	CPL	$3.54^{+6.17}_{-2.21}$	$618.76^{+107.47}_{-179.07}$	$-0.70^{+0.12}_{-0.15}$
bn130722990	−1.414–0.237	CPL	$0.14^{+0.36}_{-0.10}$	$192.76^{+50.97}_{-108.91}$	$-1.39^{+0.15}_{-0.23}$
bn130722990	−0.237–0.542	CPL	$0.46^{+0.72}_{-0.29}$	$89.80^{+5.28}_{-10.86}$	$-0.58^{+0.20}_{-0.16}$
bn130802730	−0.038–0.030	CPL	$4.58^{+10.51}_{-3.15}$	$892.60^{+134.53}_{-242.13}$	$-0.39^{+0.16}_{-0.15}$
bn130804023	−0.046–0.015	CPL	$4.59^{+9.07}_{-3.05}$	$340.72^{+76.90}_{-131.02}$	$-1.04^{+0.12}_{-0.24}$
bn130804023	−0.015–0.014	CPL	$1.15^{+3.14}_{-0.78}$	$712.08^{+157.46}_{-226.68}$	$-0.66^{+0.18}_{-0.22}$
bn130804023	−0.014–0.081	CPL	$1.45^{+4.18}_{-1.04}$	$415.95^{+88.67}_{-154.53}$	$-0.87^{+0.11}_{-0.24}$
bn130804023	0.081–0.105	CPL	$34.20^{+40.05}_{-17.42}$	$752.58^{+59.17}_{-91.91}$	$-0.17^{+0.10}_{-0.10}$
bn130804023	0.105–0.170	CPL	$1.93^{+4.59}_{-1.33}$	$290.88^{+23.81}_{-42.68}$	$-0.18^{+0.19}_{-0.12}$
bn130804023	0.748–0.829	CPL	$22.51^{+81.27}_{-17.47}$	$256.44^{+39.65}_{-112.22}$	$-1.06^{+0.15}_{-0.25}$
bn130804023	0.829–0.846	CPL	$5.96^{+10.69}_{-3.51}$	$424.48^{+77.97}_{-133.84}$	$-0.97^{+0.11}_{-0.15}$
bn130804023	0.846–0.885	CPL	$2.29^{+7.26}_{-1.62}$	$252.29^{+36.48}_{-79.68}$	$-0.79^{+0.20}_{-0.22}$

Table A1 *– continued*

GRB	Time interval	Model	Flux (10^{-6} erg s^{-1} cm^{-2})	E_p (keV)	α
bn130808253	− 0.130–0.032	CPL	$1.25^{+2.81}_{-0.88}$	$82.83^{+6.81}_{-9.51}$	$-0.54^{+0.26}_{-0.21}$
bn130912358	− 0.103–0.027	CPL	$8.19^{+6.36}_{-3.17}$	$565.43^{+126.32}_{-213.46}$	$-0.72^{+0.16}_{-0.25}$
bn130912358	− 0.027–0.027	CPL	$2.23^{+2.45}_{-1.15}$	$877.38^{+110.18}_{-152.44}$	$-0.86^{+0.06}_{-0.07}$
bn130912358	0.027–0.287	CPL	$1.18^{+4.23}_{-0.92}$	$670.90^{+102.23}_{-146.81}$	$-0.82^{+0.10}_{-0.10}$
bn130919173	− 0.021–0.005	CPL	$1.90^{+3.29}_{-1.22}$	$296.95^{+32.27}_{-86.52}$	$-0.65^{+0.17}_{-0.22}$
bn130919173	− 0.005–0.209	CPL	$0.58^{+1.66}_{-0.41}$	$99.11^{+11.58}_{-70.80}$	$-1.41^{+0.17}_{-0.35}$
bn130919173	0.664–0.767	CPL	$5.16^{+14.56}_{-3.76}$	$160.21^{+11.88}_{-30.47}$	$-0.55^{+0.19}_{-0.16}$
bn130919173	0.767–0.930	CPL	$0.19^{+0.74}_{-0.14}$	$80.41^{+6.40}_{-13.49}$	$-0.66^{+0.27}_{-0.23}$
bn131004904	− 0.213–0.590	CPL	$0.63^{+0.72}_{-0.32}$	$159.02^{+22.08}_{-62.56}$	$-1.47^{+0.10}_{-0.13}$
bn131125689	− 0.314–0.227	CPL	$0.47^{+1.35}_{-0.34}$	$135.65^{+12.47}_{-14.57}$	$-0.07^{+0.27}_{-0.20}$
bn131126163	− 0.021–0.042	CPL	$19.13^{+37.68}_{-12.01}$	$693.99^{+51.03}_{-110.44}$	$-0.02^{+0.14}_{-0.13}$
bn131126163	0.042–0.138	CPL	$7.31^{+12.46}_{-4.45}$	$760.92^{+105.63}_{-158.31}$	$-0.43^{+0.12}_{-0.13}$
bn131128629	− 1.045–0.614	CPL	$0.25^{+0.64}_{-0.18}$	$82.55^{+5.40}_{-16.04}$	$-0.57^{+0.30}_{-0.17}$
bn131209963	− 0.532–1.158	CPL	$0.60^{+0.76}_{-0.35}$	$543.68^{+121.87}_{-136.67}$	$-0.95^{+0.10}_{-0.13}$
bn131217108	− 0.165–0.538	CPL	$2.49^{+2.64}_{-1.32}$	$1346.68^{+146.14}_{-189.09}$	$-0.37^{+0.09}_{-0.09}$
bn140105065	− 0.059–0.180	CPL	$1.82^{+2.60}_{-1.02}$	$628.25^{+96.90}_{-146.44}$	$-0.73^{+0.08}_{-0.14}$
bn140105065	0.180–0.911	CPL	$0.47^{+1.23}_{-0.32}$	$425.15^{+105.36}_{-189.05}$	$-0.93^{+0.08}_{-0.22}$
bn140105748	− 0.218–0.500	CPL	$0.88^{+2.09}_{-0.61}$	$477.10^{+52.81}_{-90.14}$	$-0.30^{+0.18}_{-0.14}$
bn140129499	− 0.021–0.024	CPL	$4.26^{+9.62}_{-2.85}$	$527.83^{+83.45}_{-158.86}$	$-0.72^{+0.12}_{-0.18}$
bn140216331	− 0.376–0.724	CPL	$0.66^{+1.47}_{-0.47}$	$636.51^{+112.23}_{-151.94}$	$-0.57^{+0.15}_{-0.17}$
bn140328560	− 1.137–0.130	CPL	$0.28^{+0.85}_{-0.21}$	$219.03^{+35.67}_{-120.62}$	$-1.12^{+0.16}_{-0.25}$
bn140329272	− 0.026–0.042	CPL	$3.61^{+7.14}_{-2.40}$	$496.10^{+58.30}_{-120.01}$	$-0.50^{+0.15}_{-0.16}$
bn140402007	− 0.169–0.279	CPL	$1.47^{+3.09}_{-0.95}$	$1042.09^{+147.28}_{-147.57}$	$-0.15^{+0.17}_{-0.10}$
bn140428906	− 0.247–0.038	CPL	$7.95^{+13.30}_{-4.64}$	$250.70^{+47.21}_{-122.90}$	$-0.89^{+0.22}_{-0.28}$
bn140428906	− 0.038–0.009	CPL	$4.08^{+9.97}_{-2.83}$	$936.02^{+183.21}_{-201.62}$	$-0.60^{+0.12}_{-0.12}$
bn140428906	0.009–0.103	CPL	$0.60^{+2.79}_{-0.48}$	$797.57^{+153.52}_{-189.28}$	$-0.56^{+0.13}_{-0.19}$
bn140501139	− 0.137–0.059	CPL	$1.11^{+2.65}_{-0.81}$	$583.34^{+110.70}_{-198.50}$	$-0.64^{+0.14}_{-0.20}$
bn140511095	− 0.039–0.062	CPL	$2.76^{+4.32}_{-1.65}$	$432.28^{+65.04}_{-98.25}$	$-0.80^{+0.12}_{-0.14}$
bn140511095	0.062–0.402	CPL	$0.29^{+0.58}_{-0.18}$	$98.00^{+21.90}_{-49.60}$	$-1.54^{+0.16}_{-0.20}$
bn140605377	− 0.034–0.135	CPL	$5.14^{+6.95}_{-2.98}$	$852.53^{+83.58}_{-139.35}$	$-0.34^{+0.11}_{-0.13}$
bn140610487	− 0.230–0.114	CPL	$1.50^{+3.73}_{-1.04}$	$796.29^{+114.41}_{-197.35}$	$-0.40^{+0.15}_{-0.17}$
bn140619490	− 0.053–0.078	CPL	$2.16^{+7.86}_{-1.58}$	$284.40^{+32.11}_{-75.43}$	$-0.71^{+0.19}_{-0.25}$
bn140624423	− 0.003–0.028	CPL	$8.95^{+12.24}_{-5.12}$	$351.26^{+37.29}_{-62.77}$	$-0.67^{+0.13}_{-0.14}$
bn140710537	− 0.065–0.322	CPL	$0.98^{+3.77}_{-0.74}$	$396.48^{+58.51}_{-112.16}$	$-0.22^{+0.20}_{-0.23}$
bn140716306	− 0.597–0.532	CPL	$0.97^{+1.87}_{-0.70}$	$853.96^{+156.74}_{-191.92}$	$-0.52^{+0.11}_{-0.17}$
bn140720158	− 0.031–0.028	CPL	$3.14^{+7.28}_{-2.17}$	$603.94^{+100.90}_{-206.88}$	$-0.60^{+0.13}_{-0.20}$
bn140724533	− 0.272–0.105	CPL	$0.42^{+1.94}_{-0.32}$	$249.42^{+32.02}_{-101.77}$	$-0.78^{+0.24}_{-0.26}$
bn140807500	− 0.168–0.013	CPL	$5.67^{+3.92}_{-2.28}$	$670.15^{+136.81}_{-164.02}$	$-0.89^{+0.12}_{-0.12}$
bn140807500	0.013–0.263	CPL	$0.37^{+1.06}_{-0.26}$	$682.64^{+75.00}_{-92.84}$	$-0.74^{+0.07}_{-0.07}$
bn140807500	0.263–0.629	CPL	$1.57^{+2.43}_{-0.92}$	$296.90^{+80.93}_{-128.71}$	$-1.23^{+0.12}_{-0.24}$
bn140819160	− 0.595–0.272	CPL	$0.98^{+2.25}_{-0.67}$	$58.73^{+5.98}_{-10.63}$	$-1.19^{+0.22}_{-0.22}$
bn140819160	− 0.272–0.033	CPL	$0.07^{+0.30}_{-0.06}$	$53.53^{+12.65}_{-31.00}$	$-1.35^{+0.25}_{-0.42}$
bn140819160	− 0.033–0.043	CPL	$0.37^{+0.78}_{-0.22}$	$150.43^{+20.64}_{-33.45}$	$-0.89^{+0.19}_{-0.18}$
bn140819160	0.043–0.860	CPL	$0.09^{+0.49}_{-0.07}$	$70.94^{+16.68}_{-30.77}$	$-1.18^{+0.34}_{-0.31}$

Table A1 – *continued*

GRB	Time interval	Model	Flux (10^{-6} erg s^{-1} cm^{-2})	E_p (keV)	α
bn140831374	−0.294–1.295	CPL	$0.88^{+0.89}_{-0.44}$	$653.40^{+124.50}_{-139.23}$	$-0.89^{+0.08}_{-0.10}$
bn140901821	−0.012–0.016	CPL	$33.95^{+15.75}_{-10.75}$	$333.70^{+29.58}_{-54.43}$	$-0.44^{+0.15}_{-0.12}$
bn140901821	0.026–0.165	CPL	$1.45^{+7.03}_{-1.17}$	$1370.79^{+65.10}_{-55.13}$	$-0.12^{+0.04}_{-0.05}$
bn140901821	0.165–0.217	CPL	$11.36^{+16.39}_{-6.81}$	$148.40^{+13.72}_{-45.46}$	$-0.74^{+0.30}_{-0.26}$
bn140912664	−1.025–0.632	CPL	$0.45^{+1.06}_{-0.30}$	$398.79^{+47.34}_{-112.87}$	$-0.55^{+0.16}_{-0.18}$
bn140930134	−0.167–0.796	CPL	$0.84^{+1.47}_{-0.51}$	$646.49^{+85.13}_{-167.32}$	$-0.55^{+0.10}_{-0.16}$
bn141011282	−0.014–0.003	CPL	$10.53^{+10.30}_{-4.96}$	$785.04^{+81.77}_{-113.92}$	$-0.50^{+0.11}_{-0.09}$
bn141011282	−0.003–0.059	CPL	$0.46^{+2.69}_{-0.37}$	$611.38^{+69.48}_{-89.95}$	$-0.53^{+0.08}_{-0.10}$
bn141011282	0.059–0.111	CPL	$35.07^{+40.13}_{-19.34}$	$68.11^{+6.56}_{-27.11}$	$-1.10^{+0.22}_{-0.49}$
bn141102112	−0.032–0.007	CPL	$3.73^{+13.00}_{-2.84}$	$394.38^{+51.75}_{-146.67}$	$-0.70^{+0.20}_{-0.23}$
bn141102536	−0.060–0.009	CPL	$3.72^{+4.25}_{-1.92}$	$626.89^{+95.09}_{-181.63}$	$-0.51^{+0.14}_{-0.20}$
bn141102536	1.271–1.343	CPL	$1.46^{+1.97}_{-0.79}$	$647.01^{+138.21}_{-221.58}$	$-0.79^{+0.15}_{-0.22}$
bn141102536	1.343–1.494	CPL	$2.91^{+7.86}_{-2.08}$	$505.10^{+63.37}_{-95.34}$	$-0.74^{+0.11}_{-0.09}$
bn141102536	1.494–1.900	CPL	$1.39^{+4.28}_{-1.01}$	$735.86^{+103.49}_{-174.75}$	$-0.71^{+0.09}_{-0.12}$
bn141105406	−0.108–0.666	CPL	$1.81^{+2.09}_{-0.94}$	$431.60^{+39.75}_{-55.30}$	$-0.44^{+0.10}_{-0.11}$
bn141113346	−0.055–0.034	CPL	$1.66^{+4.35}_{-1.20}$	$572.56^{+102.86}_{-179.87}$	$-0.66^{+0.13}_{-0.22}$
bn141122087	−0.055–0.079	CPL	$2.03^{+6.10}_{-1.38}$	$614.04^{+127.97}_{-159.78}$	$-0.51^{+0.14}_{-0.19}$
bn141124277	−0.564–0.060	CPL	$0.99^{+2.49}_{-0.72}$	$557.79^{+83.82}_{-158.08}$	$-0.63^{+0.15}_{-0.19}$
bn141126233	−0.193–0.401	CPL	$0.73^{+1.69}_{-0.48}$	$660.82^{+130.52}_{-161.80}$	$-0.67^{+0.13}_{-0.17}$
bn141202470	−0.046–1.337	CPL	$3.33^{+2.42}_{-1.28}$	$626.28^{+33.93}_{-52.16}$	$-0.13^{+0.08}_{-0.07}$
bn141202470	1.337–1.756	CPL	$0.21^{+0.69}_{-0.16}$	$302.34^{+72.14}_{-195.06}$	$-1.12^{+0.16}_{-0.26}$
bn141205337	−0.082–0.695	CPL	$1.21^{+3.39}_{-0.88}$	$666.42^{+84.10}_{-157.70}$	$-0.38^{+0.16}_{-0.20}$
bn141208632	−0.954–0.057	CPL	$0.29^{+0.96}_{-0.22}$	$323.87^{+50.98}_{-136.06}$	$-0.89^{+0.17}_{-0.25}$
bn141208632	−0.057–0.025	CPL	$1.36^{+4.10}_{-0.96}$	$480.08^{+95.57}_{-176.17}$	$-0.78^{+0.13}_{-0.23}$
bn150101641	−0.016–0.002	CPL	$6.31^{+12.64}_{-3.95}$	$454.61^{+91.23}_{-120.64}$	$-0.84^{+0.11}_{-0.17}$
bn150101641	0.002–0.097	CPL	$0.31^{+1.07}_{-0.25}$	$28.75^{+5.23}_{-5.57}$	$-1.01^{+0.35}_{-0.37}$
bn150118927	−0.016–0.043	CPL	$2.30^{+3.96}_{-1.36}$	$569.47^{+56.19}_{-79.93}$	$-0.60^{+0.07}_{-0.09}$
bn150118927	0.043–0.118	CPL	$0.36^{+1.48}_{-0.26}$	$168.27^{+18.48}_{-45.74}$	$-1.03^{+0.14}_{-0.20}$
bn150118927	0.118–0.260	CPL	$15.05^{+12.01}_{-6.66}$	$125.73^{+17.94}_{-91.49}$	$-1.37^{+0.16}_{-0.30}$
bn150128624	−0.054–0.049	CPL	$2.68^{+11.09}_{-2.02}$	$360.42^{+66.80}_{-115.25}$	$-0.84^{+0.13}_{-0.31}$
bn150208929	−0.111–0.062	CPL	$2.46^{+8.59}_{-1.90}$	$747.05^{+146.12}_{-194.51}$	$-0.48^{+0.15}_{-0.23}$
bn150214293	−0.127–0.206	CPL	$1.26^{+2.41}_{-0.77}$	$666.28^{+121.85}_{-170.58}$	$-0.70^{+0.10}_{-0.16}$
bn150301045	−0.010–0.014	CPL	$3.68^{+14.06}_{-2.90}$	$186.40^{+17.04}_{-55.01}$	$-0.54^{+0.27}_{-0.23}$
bn150312403	−0.029–0.020	CPL	$2.84^{+7.24}_{-2.03}$	$287.38^{+28.18}_{-76.68}$	$-0.64^{+0.17}_{-0.23}$
bn150320462	−0.066–0.015	CPL	$9.74^{+28.60}_{-7.28}$	$932.95^{+100.01}_{-168.54}$	$-0.23^{+0.14}_{-0.18}$
bn150326521	−1.011–0.563	CPL	$0.21^{+0.71}_{-0.15}$	$111.69^{+8.94}_{-21.77}$	$-0.66^{+0.23}_{-0.25}$
bn150412507	−0.121–0.331	CPL	$0.21^{+1.12}_{-0.17}$	$88.12^{+9.83}_{-27.88}$	$-1.00^{+0.30}_{-0.33}$
bn150412931	−0.126–0.311	CPL	$1.34^{+2.86}_{-0.94}$	$677.76^{+107.66}_{-165.36}$	$-0.47^{+0.16}_{-0.15}$
bn150425617	−0.285–0.026	CPL	$0.74^{+2.42}_{-0.55}$	$874.62^{+181.02}_{-245.40}$	$-0.50^{+0.17}_{-0.19}$
bn150506630	−0.022–0.272	CPL	$3.08^{+2.74}_{-1.38}$	$935.55^{+120.61}_{-152.58}$	$-0.66^{+0.06}_{-0.11}$
bn150506630	0.272–0.841	CPL	$0.40^{+1.36}_{-0.31}$	$367.21^{+76.16}_{-129.07}$	$-0.85^{+0.18}_{-0.22}$
bn150506972	−0.204–0.196	CPL	$1.40^{+1.93}_{-0.77}$	$824.32^{+132.76}_{-188.22}$	$-0.70^{+0.08}_{-0.14}$
bn150522944	−0.148–0.263	CPL	$0.75^{+1.78}_{-0.50}$	$377.81^{+47.41}_{-125.11}$	$-0.71^{+0.16}_{-0.18}$

Table A1 *– continued*

GRB	Time interval	Model	Flux (10^{-6} erg s^{-1} cm^{-2})	$E_{\rm p}$ (keV)	α
bn150604434	−0.175–0.018	CPL	$4.67^{+6.77}_{-2.65}$	$354.56^{+92.18}_{-161.02}$	$-1.09^{+0.16}_{-0.25}$
bn150604434	−0.018–0.049	CPL	$2.54^{+2.48}_{-1.30}$	$949.39^{+154.12}_{-153.62}$	$-0.57^{+0.10}_{-0.14}$
bn150604434	0.671–0.941	CPL	$0.50^{+1.71}_{-0.36}$	$697.27^{+86.27}_{-138.23}$	$-0.72^{+0.08}_{-0.10}$
bn150605782	−0.041–0.001	CPL	$1.65^{+8.62}_{-1.32}$	$272.00^{+34.32}_{-115.25}$	$-0.86^{+0.18}_{-0.34}$
bn150609316	−0.020–0.007	CPL	$5.04^{+25.07}_{-4.05}$	$377.97^{+38.93}_{-132.27}$	$-0.41^{+0.28}_{-0.24}$
bn150628767	−0.038–0.041	CPL	$1.99^{+4.95}_{-1.50}$	$609.61^{+106.32}_{-203.71}$	$-0.53^{+0.16}_{-0.19}$
bn150628767	0.041–0.736	CPL	$0.72^{+2.05}_{-0.49}$	$652.82^{+94.54}_{-166.61}$	$-0.47^{+0.16}_{-0.17}$
bn150629564	−0.125–0.156	CPL	$2.24^{+1.96}_{-1.00}$	$1028.24^{+136.61}_{-155.92}$	$-0.83^{+0.07}_{-0.08}$
bn150705588	−0.198–0.089	CPL	$0.51^{+1.32}_{-0.33}$	$177.27^{+30.12}_{-68.52}$	$-1.21^{+0.16}_{-0.20}$
bn150715136	−0.142–0.146	CPL	$1.17^{+2.08}_{-0.76}$	$728.98^{+124.08}_{-194.71}$	$-0.66^{+0.13}_{-0.16}$
bn150721431	−0.110–0.206	CPL	$0.95^{+2.96}_{-0.74}$	$697.09^{+134.96}_{-228.95}$	$-0.63^{+0.15}_{-0.21}$
bn150728151	−0.111–0.075	CPL	$1.25^{+3.05}_{-0.86}$	$418.26^{+100.55}_{-190.49}$	$-1.18^{+0.16}_{-0.20}$
bn150728151	−0.075–0.270	CPL	$0.96^{+2.13}_{-0.63}$	$572.10^{+80.69}_{-184.20}$	$-0.61^{+0.14}_{-0.18}$
bn150728151	1.322–1.538	CPL	$1.55^{+4.21}_{-1.09}$	$423.67^{+80.76}_{-150.87}$	$-0.84^{+0.12}_{-0.20}$
bn150805746	−0.625–0.414	CPL	$0.36^{+1.68}_{-0.27}$	$84.67^{+7.26}_{-32.54}$	$-1.24^{+0.24}_{-0.32}$
bn150805746	−0.414–1.233	CPL	$0.16^{+0.55}_{-0.12}$	$61.07^{+5.13}_{-14.75}$	$-1.09^{+0.26}_{-0.35}$
bn150810485	−0.020–0.047	CPL	$7.17^{+10.77}_{-4.26}$	$523.11^{+43.70}_{-89.97}$	$-0.24^{+0.14}_{-0.10}$
bn150810485	0.047–0.417	CPL	$4.53^{+2.80}_{-1.69}$	$1367.76^{+118.05}_{-169.53}$	$-0.60^{+0.05}_{-0.07}$
bn150811849	−0.039–0.247	CPL	$9.26^{+12.92}_{-5.23}$	$1336.84^{+128.77}_{-135.49}$	$0.04^{+0.10}_{-0.08}$
bn150811849	0.247–0.456	CPL	$2.46^{+4.35}_{-1.61}$	$1416.35^{+134.85}_{-159.27}$	$-0.18^{+0.09}_{-0.09}$
bn150811849	0.456–0.530	CPL	$5.63^{+6.28}_{-3.13}$	$773.26^{+76.66}_{-145.48}$	$-0.42^{+0.10}_{-0.14}$
bn150811849	0.530–0.657	CPL	$9.52^{+9.85}_{-4.71}$	$682.56^{+125.68}_{-200.21}$	$-0.82^{+0.12}_{-0.16}$
bn150819440	−0.015–0.013	CPL	$6.62^{+3.55}_{-1.97}$	$820.85^{+161.17}_{-217.88}$	$-0.36^{+0.20}_{-0.23}$
bn150819440	−0.013–0.004	CPL	$1.99^{+0.91}_{-0.59}$	$629.45^{+44.95}_{-55.79}$	$-0.08^{+0.11}_{-0.10}$
bn150819440	0.005–0.027	CPL	$9.05^{+5.21}_{-3.01}$	$674.99^{+32.69}_{-41.71}$	$0.19^{+0.09}_{-0.08}$
bn150819440	0.027–0.058	CPL	$19.44^{+5.63}_{-3.87}$	$268.89^{+14.48}_{-18.12}$	$0.08^{+0.14}_{-0.07}$
bn150819440	0.058–0.097	CPL	$109.66^{+98.82}_{-51.26}$	$154.34^{+13.69}_{-47.52}$	$-0.87^{+0.26}_{-0.18}$
bn150819440	0.499–0.522	CPL	$23.39^{+25.96}_{-11.87}$	$60.18^{+5.77}_{-12.66}$	$-0.75^{+0.22}_{-0.38}$
bn150819440	0.522–0.545	CPL	$0.34^{+1.57}_{-0.28}$	$168.73^{+20.05}_{-34.95}$	$-1.03^{+0.05}_{-0.08}$
bn150819440	0.545–0.664	CPL	$2.75^{+2.41}_{-1.09}$	$299.90^{+19.29}_{-22.09}$	$-0.99^{+0.03}_{-0.04}$
bn150819440	0.664–0.701	CPL	$23.93^{+109.59}_{-19.30}$	$149.03^{+17.46}_{-22.30}$	$-1.07^{+0.04}_{-0.07}$
bn150819440	0.701–0.800	CPL	$1.94^{+6.97}_{-1.44}$	$69.35^{+5.97}_{-10.35}$	$-1.22^{+0.04}_{-0.09}$
bn150819440	0.800–0.950	CPL	$0.82^{+1.51}_{-0.50}$	$43.06^{+3.67}_{-6.50}$	$-1.10^{+0.14}_{-0.27}$
bn150819440	0.950–1.062	CPL	$1.09^{+2.21}_{-0.61}$	$181.58^{+45.81}_{-132.81}$	$-1.39^{+0.18}_{-0.33}$
bn150819440	1.062–1.100	CPL	$79.84^{+98.35}_{-44.40}$	$81.51^{+9.93}_{-17.77}$	$-1.13^{+0.05}_{-0.14}$
bn150819440	1.100–1.152	CPL	$3.24^{+8.07}_{-2.41}$	$88.38^{+4.47}_{-42.28}$	$-1.32^{+0.09}_{-0.21}$
bn150820880	−0.596–0.415	CPL	$0.26^{+0.73}_{-0.18}$	$339.93^{+65.24}_{-168.96}$	$-1.02^{+0.14}_{-0.21}$
bn150906944	−0.050–0.007	CPL	$18.90^{+48.84}_{-13.14}$	$578.13^{+112.90}_{-198.74}$	$-0.71^{+0.12}_{-0.19}$
bn150906944	−0.007–0.008	CPL	$0.70^{+4.51}_{-0.57}$	$758.81^{+100.43}_{-126.13}$	$-0.24^{+0.17}_{-0.14}$
bn150906944	0.008–0.130	CPL	$3.87^{+9.74}_{-2.43}$	$188.65^{+26.64}_{-93.99}$	$-0.88^{+0.23}_{-0.37}$
bn150912600	−0.184–0.284	CPL	$1.37^{+2.52}_{-0.93}$	$445.08^{+47.81}_{-78.12}$	$-0.26^{+0.17}_{-0.14}$
bn150922234	−0.021–0.008	CPL	$1.40^{+4.00}_{-0.95}$	$418.69^{+88.33}_{-162.79}$	$-0.94^{+0.13}_{-0.22}$
bn150922234	−0.008–0.058	CPL	$9.60^{+13.68}_{-5.29}$	$258.54^{+39.24}_{-93.23}$	$-1.04^{+0.16}_{-0.22}$
bn150922234	0.058–0.140	CPL	$4.39^{+10.04}_{-3.12}$	$687.30^{+53.31}_{-94.23}$	$-0.28^{+0.10}_{-0.10}$

68 per cent credible regions for the parameters of the spectra.

Table A1 – *continued*

GRB	Time interval	Model	Flux (10^{-6} erg s^{-1} cm^{-2})	E_p (keV)	α
bn150923297	−0.057–0.040	CPL	$1.49^{+2.74}_{-1.01}$	$393.02^{+82.09}_{-149.94}$	$-0.95^{+0.11}_{-0.18}$
bn150923429	0.053–0.213	CPL	$1.11^{+5.48}_{-0.88}$	$432.12^{+53.10}_{-149.56}$	$-0.52^{+0.20}_{-0.25}$
bn151022577	−0.172–0.081	CPL	$1.48^{+3.42}_{-1.00}$	$290.56^{+23.79}_{-90.15}$	$-0.76^{+0.15}_{-0.20}$
bn151222340	−0.092–0.091	CPL	$2.09^{+5.45}_{-1.45}$	$462.83^{+72.59}_{-129.41}$	$-0.77^{+0.14}_{-0.19}$
bn151222340	0.220–0.546	CPL	$5.41^{+6.78}_{-2.80}$	$1297.50^{+123.72}_{-145.19}$	$-0.39^{+0.07}_{-0.12}$
bn151228129	−0.068–0.212	CPL	$3.48^{+7.36}_{-2.47}$	$823.78^{+93.92}_{-178.01}$	$-0.31^{+0.14}_{-0.18}$
bn151229285	−0.112–0.542	CPL	$0.56^{+1.31}_{-0.36}$	$124.54^{+8.18}_{-16.80}$	$-1.11^{+0.09}_{-0.09}$
bn151229285	0.542–0.792	CPL	$0.14^{+0.46}_{-0.10}$	$83.51^{+8.87}_{-24.45}$	$-1.29^{+0.17}_{-0.25}$
bn151229285	0.792–1.636	CPL	$1.09^{+0.78}_{-0.41}$	$30.69^{+15.53}_{-15.15}$	$-1.64^{+0.17}_{-0.33}$
bn151229486	−0.046–0.119	CPL	$1.74^{+5.14}_{-1.16}$	$566.13^{+108.69}_{-195.08}$	$-0.69^{+0.12}_{-0.21}$
bn151231568	−0.301–0.026	CPL	$0.69^{+1.82}_{-0.52}$	$425.73^{+82.13}_{-159.15}$	$-0.79^{+0.16}_{-0.22}$
bn151231568	−0.026–0.283	CPL	$3.52^{+3.27}_{-1.75}$	$499.26^{+44.92}_{-76.12}$	$-0.55^{+0.08}_{-0.11}$
bn160211119	−0.385–0.279	CPL	$0.50^{+0.88}_{-0.32}$	$501.10^{+120.07}_{-150.08}$	$-0.94^{+0.12}_{-0.17}$
bn160314473	−0.035–0.080	CPL	$0.92^{+2.22}_{-0.61}$	$367.58^{+90.85}_{-167.94}$	$-1.05^{+0.13}_{-0.19}$
bn160406503	−0.028–0.062	CPL	$6.59^{+9.74}_{-3.88}$	$670.09^{+81.55}_{-133.91}$	$-0.44^{+0.13}_{-0.10}$
bn160406503	0.062–0.169	CPL	$1.10^{+3.37}_{-0.74}$	$382.62^{+72.45}_{-164.22}$	$-0.93^{+0.15}_{-0.21}$
bn160408268	−0.043–0.335	CPL	$3.30^{+2.87}_{-1.55}$	$819.49^{+91.25}_{-140.85}$	$-0.68^{+0.06}_{-0.10}$
bn160428412	−0.199–0.043	CPL	$1.18^{+2.55}_{-0.84}$	$895.82^{+142.04}_{-227.83}$	$-0.61^{+0.13}_{-0.18}$
bn160603719	−0.384–0.500	CPL	$0.77^{+1.81}_{-0.53}$	$591.43^{+101.51}_{-155.18}$	$-0.63^{+0.14}_{-0.18}$
bn160612842	−0.025–0.083	CPL	$6.50^{+7.30}_{-3.34}$	$1120.84^{+142.62}_{-185.86}$	$-0.54^{+0.08}_{-0.11}$
bn160612842	0.083–0.158	CPL	$2.17^{+6.62}_{-1.61}$	$947.71^{+201.53}_{-213.40}$	$-0.55^{+0.15}_{-0.20}$
bn160624477	−0.048–0.210	CPL	$1.89^{+3.95}_{-1.28}$	$898.54^{+135.79}_{-213.67}$	$-0.46^{+0.13}_{-0.16}$
bn160714097	−0.055–0.207	CPL	$0.57^{+1.86}_{-0.43}$	$267.49^{+35.11}_{-97.58}$	$-0.77^{+0.17}_{-0.27}$
bn160726065	−0.035–0.034	CPL	$4.62^{+3.73}_{-2.09}$	$311.54^{+43.10}_{-105.73}$	$-0.90^{+0.13}_{-0.17}$
bn160726065	0.534–0.706	CPL	$0.25^{+1.00}_{-0.20}$	$553.86^{+60.53}_{-110.18}$	$-0.75^{+0.07}_{-0.10}$
bn160726065	0.706–0.899	CPL	$2.07^{+4.41}_{-1.25}$	$162.67^{+31.53}_{-106.49}$	$-1.33^{+0.17}_{-0.30}$
bn160804180	−0.035–0.082	CPL	$16.19^{+36.54}_{-11.31}$	$627.63^{+101.04}_{-170.19}$	$-0.68^{+0.11}_{-0.15}$
bn160804180	0.082–0.310	CPL	$3.42^{+4.95}_{-2.02}$	$595.61^{+130.67}_{-210.67}$	$-0.68^{+0.14}_{-0.16}$
bn160804180	0.310–0.323	CPL	$2.90^{+5.14}_{-1.68}$	$865.30^{+116.20}_{-202.91}$	$-0.27^{+0.17}_{-0.14}$
bn160804180	0.323–0.630	CPL	$1.32^{+2.81}_{-0.85}$	$710.99^{+77.45}_{-131.62}$	$-0.34^{+0.12}_{-0.13}$
bn160804968	−0.023–0.086	CPL	$3.91^{+4.95}_{-2.10}$	$942.13^{+164.66}_{-212.74}$	$-0.64^{+0.08}_{-0.11}$
bn160806584	−0.368–0.005	CPL	$1.76^{+2.05}_{-0.97}$	$102.56^{+7.65}_{-20.16}$	$-0.46^{+0.28}_{-0.21}$
bn160806584	0.005–0.527	CPL	$0.60^{+1.40}_{-0.38}$	$172.22^{+10.23}_{-15.91}$	$-0.44^{+0.13}_{-0.12}$
bn160806584	0.527–1.131	CPL	$0.51^{+1.85}_{-0.37}$	$141.54^{+15.65}_{-33.38}$	$-1.01^{+0.17}_{-0.21}$
bn160818230	−0.167–0.252	CPL	$1.17^{+2.98}_{-0.82}$	$335.59^{+35.66}_{-100.99}$	$-0.81^{+0.16}_{-0.21}$
bn160820496	−0.059–0.284	CPL	$2.50^{+2.58}_{-1.28}$	$659.64^{+98.66}_{-124.86}$	$-0.71^{+0.08}_{-0.12}$
bn160821937	−0.040–0.096	CPL	$0.89^{+1.78}_{-0.54}$	$156.23^{+26.16}_{-72.07}$	$-1.39^{+0.10}_{-0.21}$
bn160821937	0.096–1.083	CPL	$0.12^{+0.44}_{-0.09}$	$98.25^{+13.38}_{-44.06}$	$-1.30^{+0.19}_{-0.34}$
bn160822672	−0.017–0.008	CPL	$39.47^{+45.14}_{-21.08}$	$464.20^{+93.83}_{-190.13}$	$-0.81^{+0.15}_{-0.21}$
bn160822672	−0.008–0.009	CPL	$1.49^{+8.11}_{-1.17}$	$734.63^{+57.13}_{-135.57}$	$-0.44^{+0.11}_{-0.10}$
bn160822672	0.009–0.033	CPL	$7.95^{+23.66}_{-5.81}$	$128.79^{+14.04}_{-61.48}$	$-0.98^{+0.26}_{-0.33}$
bn160826938	−0.989–0.253	CPL	$0.22^{+0.72}_{-0.16}$	$104.87^{+5.82}_{-25.32}$	$-0.61^{+0.29}_{-0.21}$
bn160829334	−0.048–0.225	CPL	$1.72^{+3.39}_{-1.18}$	$711.92^{+84.82}_{-198.10}$	$-0.45^{+0.13}_{-0.16}$

Table A1 *– continued*

GRB	Time interval	Model	Flux (10^{-6} erg s^{-1} cm^{-2})	$E_{\rm p}$ (keV)	α
bn161015400	− 0.081–0.026	CPL	$1.80^{+6.52}_{-1.28}$	$616.74^{+152.08}_{-220.23}$	$-0.60^{+0.13}_{-0.21}$
bn161026373	− 0.026–0.113	CPL	$1.52^{+3.09}_{-0.99}$	$444.36^{+72.44}_{-132.85}$	$-0.68^{+0.13}_{-0.19}$
bn161110179	− 1.458–0.261	CPL	$0.45^{+0.88}_{-0.28}$	$735.73^{+109.62}_{-204.09}$	$-0.65^{+0.10}_{-0.17}$
bn161115745	− 0.073–0.012	CPL	$1.78^{+5.48}_{-1.29}$	$592.31^{+100.45}_{-204.23}$	$-0.62^{+0.17}_{-0.18}$
bn161210524	− 0.232–0.543	CPL	$0.60^{+1.95}_{-0.44}$	$335.36^{+42.99}_{-131.30}$	$-0.75^{+0.19}_{-0.21}$
bn161212652	− 0.343–0.268	CPL	$0.97^{+3.15}_{-0.73}$	$583.45^{+96.21}_{-179.60}$	$-0.64^{+0.18}_{-0.20}$
bn161218222	− 0.040–0.167	CPL	$7.21^{+6.18}_{-3.28}$	$1742.38^{+147.06}_{-137.91}$	$-0.26^{+0.08}_{-0.06}$
bn161230298	− 0.050–0.036	CPL	$2.35^{+5.23}_{-1.63}$	$589.24^{+81.77}_{-185.58}$	$-0.70^{+0.11}_{-0.21}$
bn170111760	− 0.052–0.088	CPL	$2.31^{+5.20}_{-1.64}$	$750.33^{+138.99}_{-173.78}$	$-0.48^{+0.14}_{-0.17}$
bn170111815	− 0.667–0.112	CPL	$0.82^{+1.53}_{-0.55}$	$116.41^{+17.62}_{-64.82}$	$-1.30^{+0.18}_{-0.35}$
bn170111815	− 0.112–0.375	CPL	$0.09^{+0.36}_{-0.06}$	$162.26^{+12.92}_{-36.10}$	$-0.69^{+0.18}_{-0.19}$
bn170121133	− 0.048–0.039	CPL	$3.39^{+12.96}_{-2.80}$	$634.15^{+78.70}_{-173.09}$	$-0.20^{+0.25}_{-0.21}$
bn170124528	− 0.041–0.260	CPL	$1.31^{+3.51}_{-0.91}$	$483.40^{+98.11}_{-154.17}$	$-0.66^{+0.13}_{-0.20}$
bn170127067	− 0.007–0.020	CPL	$56.00^{+32.93}_{-22.39}$	$826.94^{+43.87}_{-66.38}$	$-0.09^{+0.13}_{-0.12}$
bn170127067	0.020–0.114	CPL	$16.36^{+46.82}_{-11.72}$	$941.63^{+30.10}_{-27.17}$	$0.23^{+0.07}_{-0.04}$
bn170127067	0.114–0.158	CPL	$63.80^{+114.75}_{-41.27}$	$592.85^{+40.21}_{-93.27}$	$-0.18^{+0.17}_{-0.17}$
bn170127634	− 0.032–0.010	CPL	$4.83^{+7.58}_{-3.01}$	$656.15^{+104.29}_{-169.42}$	$-0.77^{+0.09}_{-0.17}$
bn170127634	0.010–0.298	CPL	$1.24^{+3.57}_{-0.92}$	$555.36^{+73.85}_{-167.55}$	$-0.39^{+0.19}_{-0.18}$
bn170203486	− 0.072–0.184	CPL	$0.89^{+2.44}_{-0.62}$	$464.42^{+111.17}_{-182.60}$	$-0.92^{+0.12}_{-0.22}$
bn170205521	− 0.219–0.117	CPL	$0.80^{+0.24}_{-0.18}$	$188.50^{+53.88}_{-129.38}$	$-1.38^{+0.17}_{-0.26}$
bn170205521	− 0.117–0.843	Band	$1.05^{+1.77}_{-0.64}$	$29.64^{+2.10}_{-5.65}$	$-1.00^{+0.33}_{-0.26}$
bn170205521	0.843–1.238	CPL	$0.50^{+1.47}_{-0.37}$	$27.09^{+5.36}_{-6.12}$	$-1.36^{+0.18}_{-0.30}$
bn170219002	− 0.040–0.013	CPL	$19.77^{+39.10}_{-12.58}$	$899.34^{+142.08}_{-202.81}$	$-0.57^{+0.14}_{-0.14}$
bn170219002	0.013–0.041	CPL	$0.71^{+2.71}_{-0.54}$	$1189.20^{+134.04}_{-159.05}$	$-0.37^{+0.10}_{-0.15}$
bn170219002	0.041–0.216	CPL	$8.21^{+20.10}_{-5.37}$	$344.81^{+93.24}_{-168.31}$	$-1.03^{+0.19}_{-0.25}$
bn170222209	− 0.028–0.013	CPL	$6.11^{+22.01}_{-4.50}$	$510.30^{+72.70}_{-123.97}$	$-0.76^{+0.09}_{-0.17}$
bn170222209	0.013–0.447	CPL	$0.63^{+1.30}_{-0.41}$	$827.67^{+63.81}_{-105.81}$	$-0.25^{+0.12}_{-0.09}$
bn170222209	0.563–1.168	CPL	$4.21^{+5.35}_{-2.31}$	$818.54^{+58.42}_{-96.38}$	$-0.26^{+0.10}_{-0.10}$
bn170222209	1.168–1.214	CPL	$4.23^{+4.58}_{-2.24}$	$689.81^{+100.03}_{-156.90}$	$-0.40^{+0.18}_{-0.18}$
bn170222209	1.214–1.910	CPL	$6.84^{+10.59}_{-4.19}$	$493.23^{+96.64}_{-162.60}$	$-0.98^{+0.11}_{-0.17}$
bn170302166	− 0.702–0.447	CPL	$0.32^{+0.54}_{-0.19}$	$71.38^{+6.87}_{-19.03}$	$-1.52^{+0.15}_{-0.22}$
bn170304003	− 0.010–0.102	CPL	$1.73^{+2.90}_{-1.01}$	$115.51^{+10.26}_{-19.74}$	$-0.90^{+0.17}_{-0.15}$
bn170304003	0.102–0.285	CPL	$0.21^{+0.98}_{-0.17}$	$27.82^{+5.18}_{-10.52}$	$-1.28^{+0.31}_{-0.45}$
bn170305256	− 0.022–0.107	CPL	$1.84^{+2.87}_{-1.13}$	$339.78^{+18.57}_{-30.15}$	$-0.31^{+0.09}_{-0.08}$
bn170305256	0.107–0.282	CPL	$0.34^{+1.26}_{-0.26}$	$178.41^{+14.34}_{-21.86}$	$-0.46^{+0.15}_{-0.16}$
bn170305256	0.282–0.627	CPL	$6.97^{+5.94}_{-3.11}$	$138.20^{+21.11}_{-72.46}$	$-1.27^{+0.19}_{-0.31}$
bn170325331	− 0.051–0.091	CPL	$2.70^{+4.97}_{-1.70}$	$837.89^{+149.28}_{-196.61}$	$-0.46^{+0.12}_{-0.15}$
bn170403583	− 0.034–0.051	CPL	$4.74^{+7.63}_{-2.80}$	$648.25^{+101.55}_{-181.59}$	$-0.80^{+0.09}_{-0.14}$
bn170403583	0.051–0.393	CPL	$0.42^{+2.06}_{-0.32}$	$161.10^{+19.09}_{-81.28}$	$-1.12^{+0.20}_{-0.31}$
bn170817529	− 0.319–0.327	CPL	$0.40^{+0.28}_{-0.18}$	$297.50^{+63.94}_{-149.55}$	$-1.06^{+0.17}_{-0.22}$
bn170818137	− 0.064–0.135	CPL	$0.97^{+1.79}_{-0.63}$	$105.80^{+7.89}_{-15.83}$	$-0.41^{+0.22}_{-0.17}$
bn170818137	0.135–0.375	CPL	$0.24^{+1.05}_{-0.19}$	$58.25^{+6.13}_{-32.83}$	$-1.38^{+0.21}_{-0.40}$

This paper has been typeset from a TEX/LATEX file prepared by the author.